Charles University in Prague, First Faculty of Medicine

Nucleolus and its Associated Chromatin

PhD Thesis

Prague 2008 **Zuzana Cvačková**

ACKNOWLEDGEMENTS

I would like to thank my supervisor Professor Ivan Raška for his continuous support, possibility to work on an interesting project and constructive criticism and help during the preparation of the thesis. Many thanks belong to David Staněk for his guidance and permanent encouragement. There are many present and former members of the lab to who belong my acknowledgements, especially to Martin Mašata for help with data analysis, Ondřej Šebesta and Jan Malínský for consultation of confocal microscopy techniques and Jana Šmigová for stimulation in every-day work.

My research work during PhD studies was markedly enriched during two fellowships abroad and many thanks belong to Karla Neugebauer and Robert Hock and to members of their laboratories.

I express my gratitude to my parents and friends for their support. Finally and most importantly I thank my husband for his high level of tolerance, support and encouragement.

This work was supported by grants from the Czech Ministry of Education MSM0021620806, LC535, from the Academy of Sciences of the Czech Republic AV0Z50110509, the Wellcome Trust grant 075834/04/Z and from the Grant agency of the Czech Republic 303/03/H065.

LIST OF ABBREVIATIONS

ATP	adenosine triphosphate
BrdU	5-bromo-2´-deoxyuridine
BSA	bovine serum albumine
CCD	charge-coupled device (camera)
c-Myc	transcriptional factor
CT	chromosome territory
DAPI	4,6-diamino-2-phenylindole dichloride
FISH	fluorescence *in situ* hybridization
FITC	fluorescein isothiocyanate
FRAP	fluorescence recovery after photobleaching
GFP	green fluorescent protein
GST	glutathione S-transferase
HeLa	human cells, derived from adenocarcinoma cervix cells
HEPES	4-(2-hydroxyethyl)-1-piperazineethanesulfonic acid
HepG2	human hepatocellular liver carcinoma cell line
ICD	interchromatin domain
ICN	interchromosomal network
LSCM	laser scanning confocal microscope
NAC	nucleolus-associated chromatin
NOR	nucleolus organizer region
PBS	phosphate buffered saline
PMT	photomultiplier tube
PNB	prenucleolar bodies
RNP	ribonucleoprotein particle
snoRNP	small nucleolar ribonucleoprotein particle
SDS-PAGE	sodium dodecyl sulphate polyacrylamide gel electrophoresis
STED	stimulated emission depletion
TIRF	total reflection fluorescence
TRITC	tetramethyl rhodamine isothiocyanate
UBF	upstream binding factor
WFM	wide-field microscope

CONTENTS

1. OUTLINE OF THE THESIS

The thesis represents a part of a research performed at the Institute of Cellular Biology and Pathology, First Faculty of Medicine, Charles University in Prague. This research is focused on the gene expression and structure-function organization of the cell nucleus, especially to dynamic organization of chromatin in relation to RNA and DNA synthesis.

This first chapter, which is preceded by the Contents and the List of abbreviations, delineates the outline of the thesis. In the chapter 2 (Theoretical background), a general introduction about the cell nucleus, chromatin and nuclear bodies is given with emphasis on the structure-function aspects of chromatin and nucleolus. Hand in hand with acquiring the new knowledge about the nucleus comes the progress of experimental technologies, particularly the live cell imaging. Accordingly, I also provide an overview of the advanced microscopy technologies, the fluorescent proteins used for imaging with special focus on the top of the line „optical highlighter fluorescent proteins“ and also some specific aspects of the live cell imaging. In the next chapter specific aims of the thesis are formulated. In the chapter 4, the material and methods employed in this thesis are shortly commented. The results of my experimental work are presented in the chapters 5 and 6. The chapter 5 is dedicated to chromatin organization in the cell nucleus and specifically to a propagation of chromatin arrangement from mother to daughter cell nuclei. This study was accepted for publication in the Journal of Structural Biology. My contribution to this work includes mainly: long-term live cell imaging (fusion protein and stable cell line preparation, chromatin labeling in living cells) and also fluorescent *in situ* hybridization and Western blot experiments. The figures accompanying the chapter 5 and 6 are provided at the end of the chapter 5 and 6, respectively. At the end of the chapter 5 there is also a commentary to the movie, which is enclosed to thesis on a CD. In the chapter 6, results of the project regarding the Pontin protein are documented. Different experimental approaches are used to localize this protein within the nucleolus and also a putative Pontin function in the nucleolus is proposed. This study arose from the collaboration with the Institute of Laboratory Medicine and Pathobiochemistry in Berlin and was published in the Chromosoma journal (Cvačková et al., 2008). I contributed here with immunofluorescence labeling (and double-labeling for purpose of colocalization

studies), nucleolar fraction preparation, Western blot analysis, siRNA experiments, immunoprecipitation and transcription labeling experiments. The results of the research described in the chapters 5 and 6 are generally discussed in the consecutive chapter 7; in this chapter also some possible directions for future research are suggested. In the chapter 8 the main conclusions of the thesis are provided. The chapter 9 summarizes the experimental studies of this thesis. The references are listed at the end of the thesis (chapter 10).

I emphasize that this thesis is focused on the investigation of mammalian, specifically human cells.

2. THEORETICAL BACKGROUND

2.1 The cell nucleus of high eukaryotes

In mammalian cells, the genetic material of the organism is "guarded" in a complex and dynamic organelle - the nucleus. Major cellular events take place there, such as DNA replication, repair and recombination, RNA synthesis and processing and ribosome subunit biogenesis. The nucleus has a unique architecture. It is enwrapped with a double-membrane nuclear envelope, which is linked to the endoplasmic reticulum on the outer side and associated with the nuclear lamina on the inner side. Large multiprotein nuclear pore complexes, that allow movement of molecules between nucleus and cytoplasm, "punctuate" nuclear envelope. Nucleus breaks down during mitosis and reforms again in nascent daughter cells.

2.1.1 Chromatin structure and organization within the nucleus

DNA is highly packed through its association with histone proteins forming nucleosomes and further compacted into higher order structures (Bednar et al., 1998). The nucleosome is the basic unit of chromatin and is composed of an octamer of the four core histones (H2A, H2B, H3 and H4) around which 147 base pairs of DNA are wrapped (Fig. 1.1a,b). Nucleosomes are incorporated into DNA during replication. DNA is first wrapped around the H3-H4 tetramer before the addition of two H2A-H2B dimers. Linker histone H1 binds to the extranucleosomal DNA. Investigation of the nucleosome assembly and histone dynamics in living cells was enabled due to successful expression of histone fused to fluorescent proteins. Kanda and his co-workers showed that histone H2B tagged to GFP is properly incorporated into chromatin and that the cell growth is unaffected by its expression (Kanda et al., 1998). Fluorescent recovery after photobleaching (FRAP) experiments revealed continual exchanging of histone H1 with residence time of few minutes irrespective of whether it is within heterochromatin or mitotic chromosome (Lever et al., 2000; Misteli et al., 2000). Exchange of core histones was studied by Kimura and Cook (2001). They showed by FRAP experiments that more than 80 % of H3-GFP and H4-GFP remained bound in nucleosomes stably. By contrast about 3 % of H2B-GFP exchanged within minutes and ~40 % exchanged slowly. Therefore inner core of the nucleosome is very stable, whereas H2B histones on the surface of nucleosomes are less stable.

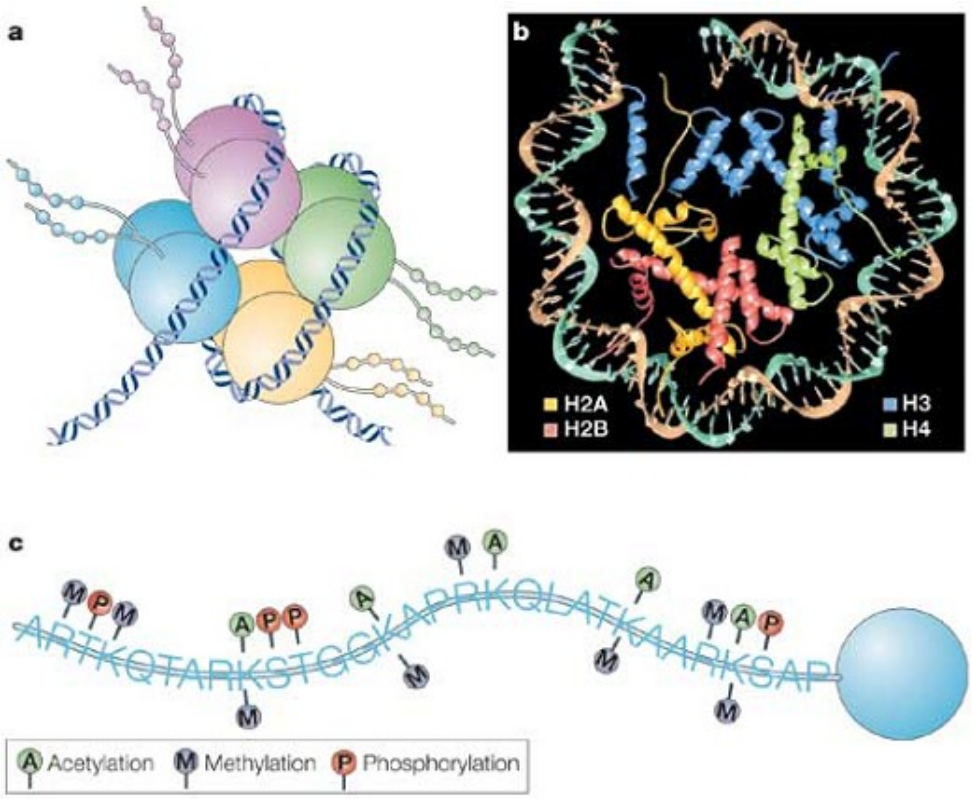

Figure 1.1 Nucleosome structure. (a) Each nucleosome consists of an octamer of histone molecules ($H3_2$-$H4_2$ tetramer and two H2A-H2B dimers). (b) Crystal structure depicts the interaction of DNA with histones. (c) The first 30 amino acids in the N-terminus of the human H3 are shown. Many sites here can be targets for epigenetics modifications (e.g. acetylation, methylation or phosphorylation). Adopted from Levenson and Sweatt (2005).

Core histones have hydrophobic, globular domains on their C- and N-terminal tails that emanate from the nucleosome octamer (Fig. 1.1a). Histone tails are characteristic by the large number and type of potentially modified residues they possess (Fig. 1.1c). These post-translation modifications include acetylation of lysines, methylation of lysines and arginines, phosphorylation of serines and threonines, ubiquitinilation and sumoylation of lysines, ADP ribosylation of glutamic acid, deimination of arginines and proline isomerization (reviewed in Kouzarides, 2007). There are two characterized mechanisms for the function of modification, (i) disruption of contacts between nucleosomes in order to unravel chromatin and (ii) recruiting of nonhistone proteins. For example, chromatin might be compacted due to acetylation of lysine residues. Acetylation neutralizes the basic charge of the lysine, which has structural consequence for the chromatin structure. Phosphorylation is another modification that may have important consequences for chromatin compaction via charge changing.

The most obvious functions that have been associated with histone tails modifications are transcription, repair and replication. Most modifications have been found to be dynamic and many enzymes that add and remove modifications have been identified. One exception is an enzyme that demethylates arginines, which has not yet been found (Kouzarides, 2007).

Besides DNA methylation, nucleosomes appear to be the major carriers of epigenetically inherited information. Local concentration and combination of differently modified nucleosomes, termed the "histone code", permit an assembly of different epigenetic states. This leads to distinct "readouts" of the genetic information, such as gene activation versus gene silencing, or more globally cell proliferation versus cell differentiation (Jenuwein and Allis, 2001).

Different histone variants having different localization and dynamics were described that. For example, histone H3 is replaced in transcriptionally active chromatin regions by its H3.3 variant in *Drosophila* (Ahmad and Henikoff, 2002). In higher eukaryotic cells, histone H2A.X is a variant having unique C-terminal amino acid extension containing serine residue, which becomes phosphorylated when DNA double strand breaks occur (Redon et al., 2002). Phosphorylated H2A.X is called γ-H2A.X and can be considered as a marker of DNA damage (Loizou et al., 2006).

Complex of DNA, histones and other non-histone proteins is termed chromatin. Most highly condensed regions of interphase chromatin are termed heterochromatin and they are often found at the nuclear periphery and in the nucleolar vicinity. Heterochromatin comprises regions in which no or little gene expression occurs and where the DNA is replicated during late S-phase stage of the cell cycle. In contrary, euchromatin consists of less condensed transcriptionaly active regions found more toward the nuclear interior (Fig. 1.2); reviewed by e.g., Mateos-Langerak et al. (2007). However, these definitions cannot be taken absolutely. For example, a DNase-sensitive and most probably transcriptionally active chromatin domain was found at the nuclear periphery (Chan et al., 2000); this indicates that the nuclear periphery might function as a compartment for spatial coupling of transcription and nucleocytoplasmic transport. An inverted pattern of chromatin organization in rod cell nuclei of mouse and other mammalian species with nocturnal vision is another exception from the rule. The constitutive heterochromatin in the center of nucleus is surrounded by the facultative heterochromatin, while

euchromatin is found at the nuclear periphery (T. Cremer, invited lecture at the Institute of Cell Biology and Pathology, Prague, 2008).

Transition between hetero- and euchromatin states can also be mediated by ATP-dependent chromatin remodeling. ATP-dependent chromatin remodeling complexes contain ATPases of the Swi/Snf superfamily and alter DNA accessibility of chromatin in an ATP-dependent manner. Examples of these complexes are evolutionary conserved INO80 and SWR1 that have been implicated in transcription regulation and DNA repair (Bao and Shen, 2007).

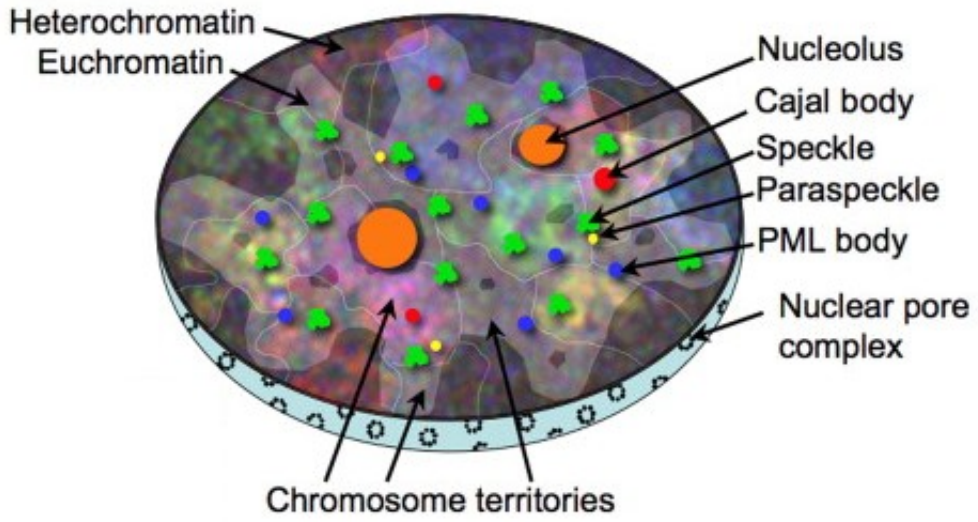

Figure 1.2 Spatial organization of the interphase nucleus: schema of global chromatin organization and subnuclear compartments arrangements. Adopted from Trinkle-Mulcahy and Lamond (2008).

In higher eukaryotic cells, DNA is physically divided into individual chromosomes that are maximally condensed during metaphase (Fig. 1.3). Arrangement of chromosomes in the cell nucleus was already studied at the turn of 19th and 20th century (Boveri, 1909; Rabl, 1885). Only much later, it was shown that chromosomes in interphase nuclei occupy mutually exclusive volumes, referred to as chromosomal territories (CTs), (Cremer and Cremer, 2001; Visser and Aten, 1999) (Fig. 1.2, 1.3). Besides other approaches, this was clearly shown by FISH painting on fixed cells (Pinkel et al., 1986; Schardin et al., 1985) and by *in vivo* experiments (Zink et al., 1998). CTs contain distinct chromosome arm domains and smaller chromatin domains with DNA content in the order of 1Mbp. These domains might assemble different sets of factors (for replication, transcription or repair) at different

times during the cell cycle and thus provides a high level of chromatin structure-function organization (Cremer and Cremer, 2001).

Number of experiments with vertebrate cells showed that the CTs are non-randomly arranged within the nuclear space (Parada and Misteli, 2002). CTs are organized radially according to their gene density (Boyle et al., 2001; Bridger et al., 2000; Cremer et al., 2003; Cremer et al., 2001; Croft et al., 1999; Tanabe et al., 2002) and according to their size (Bolzer et al., 2005; Bridger et al., 2000; Cremer et al., 2001; Sun et al., 2000). CTs were reported to have non-random neighborhoods; they occupy preferential positions relative to each other (Nagele et al., 1999; Parada et al., 2002). Several contacts between different chromosomal loci have been reported, which may contribute to gene silencing or activation. These so called "chromosome kissing" (reviewed in Cavalli, 2007) may have also important implications for chromosomal translocations (Branco and Pombo, 2006; Nikiforova et al., 2000; Roix et al., 2003); reviewed in Meaburn et al. (2007).

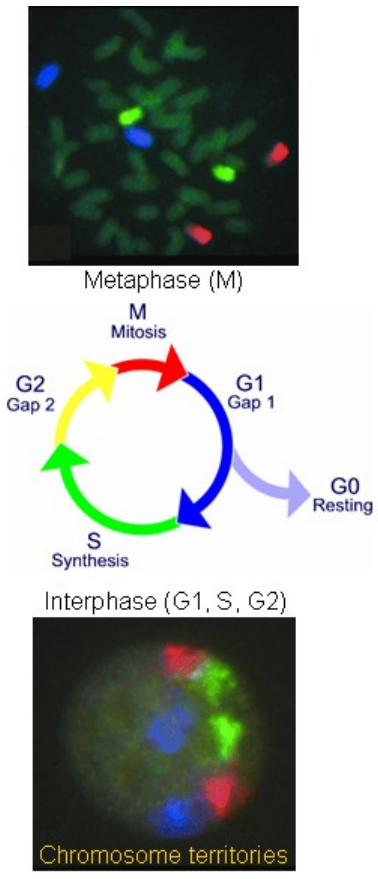

Figure 1.3 Chromosomal arrangement during the cell cycle. Metaphase spread and interphase cell nucleus are shown. Three different pairs of chromosomes are labeled by FISH.

Non-random arrangement of CTs raises the question how stringently chromosomal patterns are maintained during the cell cycle and how are propagated through mitosis to subsequent cell generations. *In vivo* labeling of chromatin and following the cells through mitosis to its descendents can only address this issue. Advanced imaging technologies nowadays enable for such experiments (see chapter 2.2). Distribution of labeled chromatin in mother and their daughter cells was studied by several groups (Essers et al., 2005; Gerlich et al., 2003; Walter et al., 2003). Chapter 5, which is dedicated to CT maintenance issue, broadens out these studies. A new aspect of our contribution is the investigation of the functionally relevant nucleolus-associated chromatin and its positioning in daughter cell nuclei (see chapter 5).

Regardless of their transcriptional activity, genes could be found anywhere within a CT (Belmont et al., 1999) and active gene regions can even loop out from CTs (Volpi et al., 2000; Williams et al., 2002). It was shown that active genes from different CTs located on decondensed chromatin loops are transcribed by the RNA polymerase II in nuclear compartments called “transcriptional factories” (Osborne et al., 2004).

One of the proposed models of chromatin/chromosome arrangement considers an existence of three nuclear compartments; an “open” chromatin compartment with chromatin domains containing active genes, a “closed” chromatin compartment consisted of inactive genes and an interchromatin domain (ICD) (Cremer et al., 2000). The ICD compartment is rich of macromolecular complexes for transcription, splicing, DNA replication and repair. According to this model, chromatin from different chromosomes is separated by an ICD, while active genes are found in direct contact with the ICD.

Recent development of the high-resolution FISH technique revealed significant intermingling of CTs during interphase, indicating that they interact more than was thought previously (Branco and Pombo, 2006). This observation led to a small rectification of the ICD model and to the proposal of the interchromosomal network (ICN) model of chromatin organization. In the ICN model, chromatin from different chromosomes is not separated, but allowed to expand to the adjacent chromosomal territories. CTs intermingle mostly at their boundaries. Intra- and interchromosomal interactions are likely to depend on the transcriptional activity of

given loci and shape chromosome organization in mammalian cells (Branco and Pombo, 2006).

2.1.2 Nuclear bodies

Cell nucleus contains distinct nuclear bodies such as Cajal bodies, Gems, nuclear speckles, paraspeckles, PML (promyelocytic leukemia) bodies, PcG bodies or the most prominent ones – the nucleoli (Fig. 1.2); reviewed in Spector (2001). Despite of the fact that these nuclear sub-organelles are not surrounded by membrane from the surrounding space, they can be classified as compartments for several reasons (Dundr and Misteli, 2001): (i) They contain a characteristic subset of resident proteins; (ii) they can be morphologically identified by light and electron microscopy and (iii) some compartments can be biochemically isolated in an enriched form. An important attribute of most nuclear bodies is continuous and rapid exchange of its resident proteins, which was probed by selective bleaching of these proteins fused to fluorescent proteins using FRAP; reviewed in Dundr and Misteli (2001). The generation of stable configurations from highly dynamic components is consistent with a role of self-organization as the driving force in generation of nuclear architecture (Misteli, 2001).

Nuclear bodies are linked with a particular nuclear function and often associate with multiple chromosomal sites (Parada and Misteli, 2002). Cajal bodies are frequently associated with U2 and histone genes (Frey et al., 1999; Schul et al., 1999); PML (promyelocytic leukemia) bodies with MHC locus on chromosome 6 (Shiels et al., 2001), the OPT (Oct1/PTF/transcription) domain with chromosomes 6 and 7 (Pombo et al., 1998) and heat shock bodies are often found near chromosomes 9, 12 and 15 (Denegri et al., 2002; Jolly et al., 2002). The nucleolus is a special example of nuclear body-chromosomal loci associations (Kalmárová et al., 2007; Smetana, 2002; Smirnov et al., 2006).

2.1.3 The multifunctional nucleolus

The nucleolus is the most obvious internal nuclear compartment that was first observed more than 200 years ago (rewieved by e.g., Busch and Smetana, 1970). Difference in the density between the nucleolus and the nucleoplasm results in the clear visibility in live cells viewed by phase contrast or DIC (differential interference contrast**)** optics. Most mammalian cells contain one to several nucleoli.

Nucleolus plays important role in ribosomal genes transcription, pre-rRNA processing and ribosome subunit assembly. rDNA is unique in the sense that ribosomal genes are highly redundant in eukaryotic genomes. There are approximately 400 copies of ribosomal genes in human diploid genome, which are arranged in arrays of head-to-tail tandem repeats separated by intergenic non-transcribed spacers (Fig. 1.4). These arrays of ribosomal genes are termed nucleolar organizer regions (NORs). In human cells, they are located on the short arms of acrocentric chromosomes 13, 14, 15, 21 and 22 and each of these chromosomes harbors 30-50 repeats per chromosome (cited by Koberna et al., 2002). Eukaryotic ribosomal genes code for three of the four rRNA molecules found in ribosomes: 18S, 5.8S and 28S rRNA. These three RNAs result from the processing of a primary transcript, the 45S rRNA precursor (Fig. 1.4). The remaining one - 5S rRNA is transcribed by RNA polymerase III in the nucleoplasm.

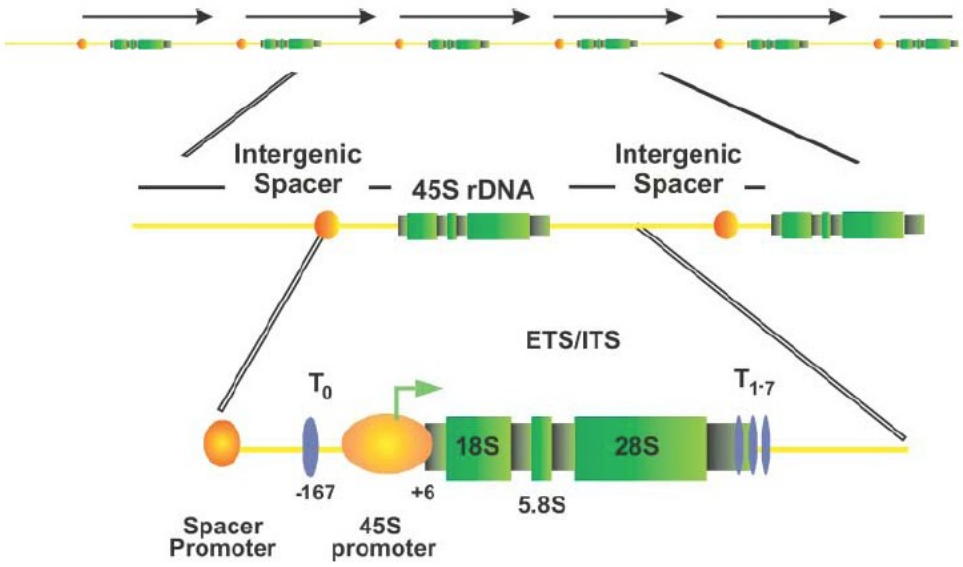

Figure 1.4 Mammalian ribosomal DNA repeats organization. Adopted from Huang et al. (2006).

As revealed by electron microscopy, the nucleolus is compartmentalized into three regions termed fibrillar centers, dense fibrillar components and granular components (Fig. 1.5). These distinct areas reflect the vectorial process of ribosome biogenesis, which is the primary function of the nucleolus. Nucleolar fibrillar centers contain proteins involved in rRNA transcription; however, rRNA genes, that are accommodated in this nucleolar subcompartemnt, are mostly transcriptionally inactive. Transcription of ribosomal DNA (rDNA) genes into precursor rRNAs (pre-

RNAs) by a specialized RNA polymerase - RNA polymerase I (pol I) occurs at the border between the fibrillar centers and the dense fibrillar components and in the dense fibrillar components (Koberna et al., 2002). Maturation of the pre-rRNA into rRNA includes cleavage and modification by the small nucleolar RNPs (snoRNPs) and other processing enzymes. Fibrillarin is a well known protein that associates with C/D box snoRNPs, which function in site-specific 2`-O-methylation of pre-rRNA. Pre-rRNA processing and pre-ribosomal assembly takes place in the dense fibrilar components and in the surrounding granular components. The 5.8S and 28S rRNAs assemble with the 5S rRNA transcript to form the 60S ribosome subunit, whereas the 18S rRNA alone assembles into the 40S subunit (Fig. 1.6). Both ribosomal subunits are than transported into cytoplasm, where they bind to the mRNA to form functional ribosomes; reviewed in Boisvert et al. (2007).

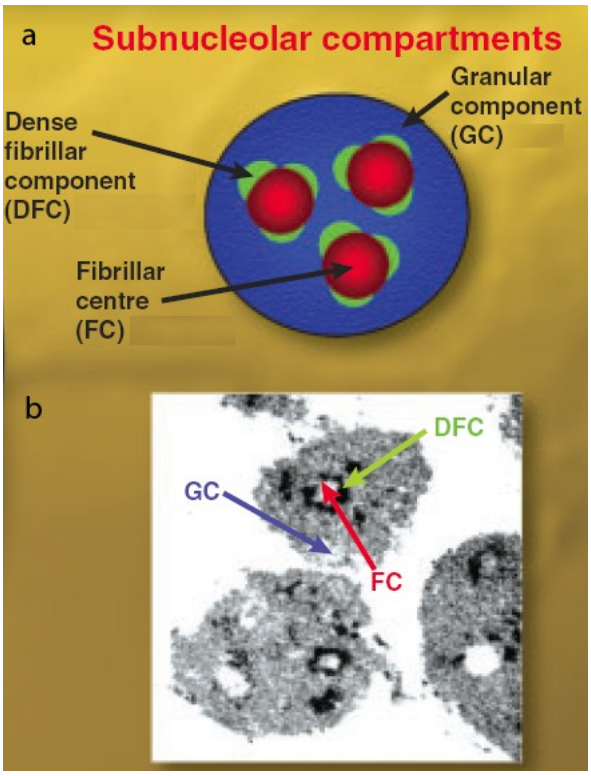

Figure 1.5 Subnucleolar compartmentalization. (a) Schematic drawing of fibrillar centers, dense fibrillar components and granular components organization within the nucleolus. (b) Transmission electron micrograph of isolated nucleoli with marked of these three sub-compartments. Adopted from Lam et al. (2005).

In mammalian cells, rDNA gene promoter contains two important sequences: upstream control element and core promoter that enables the formation of a transcriptionaly active complex (reviewed in Raška et al., 2004). This complex consists of upstream binding factor of polymerase I (UBF), selectivity factor protein complex SL1 (formed of TATA-binding protein and three transcription activating factors), transcription initiation factors TIF-IA and TIF-IC. The role in rDNA transcription termination plays the transcription termination factor TTF-1, which also acts in remodeling of ribosomal chromatin leading to silencing of rRNA genes (Santoro et al., 2002).

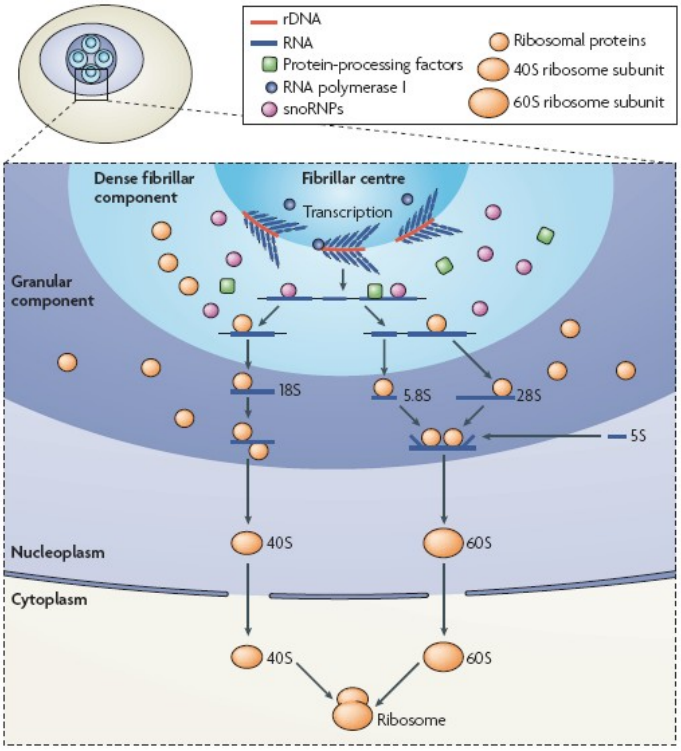

Figure 1.6 Model of ribosome biogenesis. Adopted from Boisvert et al. (2007).

Molecular organization of ribosomal transcripts was originally described on spreads of nuclear contents from amphibian oocytes (Miller and Beatty, 1969) and is referred to as "Christmas trees" (Fig. 1.7). It should be noted that such images of spread preparation were achieved with mammalian cells only exceptionally due to the interference of nuclear chromatin. rDNA repeats are fully extended (forming a trunk of this imaginary tree) and along this central DNA axis, nascent growing rRNA transcripts protrude from each rDNA unit (as branches). At the 5´ends of nascent

rRNA occur RNP particles called terminal knobs. As transcription proceeds from the initiation point, the rRNA transcripts become increasingly longer, resulting in this "Christmas tree" model.

rDNA transcription is believed to be the rate-limiting step in the process of ribosome biogenesis and it is regulated at two levels: chromatin competence and transcription initiation/elongation. Only a subset of the rDNA repeats is actively transcribed at any given time. In contrary to genes transcribed by RNA polymerase II, which are generally in two states of chromatin (actively transcribing euchromatin or silent heterochromatin), ribosomal chromatin can be found in three states (Huang et al., 2006). rDNA can be in an inactive state (similar to the heterochromatin) or in two open euchromatic states including transcriptionally competent but not active and transcriptionally productive states.

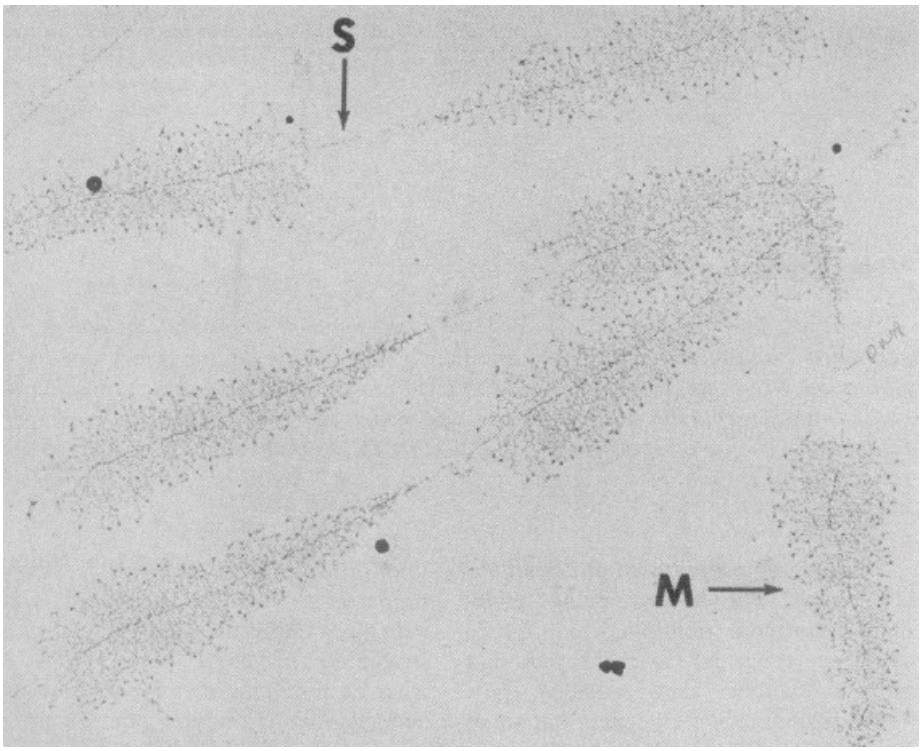

Figure 1.7 A micrograph showing transcription of ribosomal genes in amphibian oocytes. "M" points at matrix units (transcribed ribosomal genes), "S" indicates intergenic spacer sequence. Adopted from Miller and Beatty (1969).

Nucleolus as a dynamic structure undergoes disassembly during mitosis onset and reassembly at exit of mitosis (Hernandez-Verdun et al., 2002; Leung et al., 2004). During mitosis, ribosomal genes (rDNA), that are active in the previous

interphase, are arranged in partially condensed form at the NORs. These NORs are visible on chromosomes as secondary constrictions. Some proteins of the polymerase I (pol I) transcriptional machinery remains attached to the mitotic NORs. In late telophase the pol I transcription is reinitiated (Chen et al., 2005), and other nucleolar components are recruited to transcription sites so that new nucleoli are formed in early G1 phase of the next interphase. The formation of the nucleolus is done by cooperative interactions between different NOR-bearing chromosome territories (Savino et al., 2001).

Recent studies show that the function of nucleolus is not restricted only to its "classical" role in generating ribosomal subunits. Nucleolus participates in many other important cell processes such as cell cycle control, stress response, coordination of the biogenesis of other classes of functional RNPs, nuclear export, assembly of the signal recognition particle, DNA damage repair or telomere metabolism (Boisvert et al., 2007; Raška et al., 2006a). Recently, it was shown that the oocyte nucleolar material is essential for successful early embryonic development in mammals (Ogushi et al., 2008). There is a close relation between the nucleolus and human diseases, including inherited genetic disorders and predisposition to cancer (Boisvert et al., 2007; Raška et al., 2006a). In oncology, the morphology of nucleoli (size, shape, staining properties) has been used for the cytological diagnosis of malignancy since 19th century (rewieved by Busch and Smetana, 1970; Smetana, 2002).

Combination of unique density and robust structure make the nucleolus to be most convenient subnuclear structure to purify. Possibility to purify nucleoli in large scale together with high throughput mass spectrometry-based proteomic techniques identified over 3000 human proteins that stably co-purify with isolated nucleoli (Lamond, personal communication, 2008; Leung et al., 2006). Majority of identified nucleolar proteins were ribosomal proteins, RNA modifying enzymes and related proteins, RNA and DNA binding proteins, RNA helicases, transcription and splicing-related factors, and many others listed in the nucleolar protein database (http://www.lamondlab.com/NOPdb/NPDdatabase.htm). Availability of human nucleolar proteome together with bioinformatics studies brought new insights into nucleolar structure, function and also evolution of this organelle (Lam et al., 2005).

Pontin is an example of protein included in this nucleolar database to which the chapter 6 is dedicated. It was described as a putative mammalian DNA-helicase

belonging to the family of AAA+ ATPases. Pontin has also function in many cellular processes such as transcription regulation and regulation of small nucleolar ribonucleoprotein particles (snoRNP) maturation; it was also described as a component of different chromatin remodeling complexes (Cvačková et al., 2008; Gallant, 2007).

2.2 Emerging technologies for nuclear organization and dynamic studies

Our current understanding of the structure and function of the cell nucleus are from a large extent derived from methods that statistically analyze investigated features of cell populations. This is essential and indeed many of nature's secrets were revealed using fixed cells. However, some information obtained by this approach may be limited and even misleading as we need to study nuclear processes at the single cell level and, even more importantly, also perform live cell investigations. An improvement of microscope optical design, development of new fluorochromes, progress of *in vivo* labeling techniques and use of advanced softwares open new possibilities of live cell imaging which became a commonly used approach of the modern cell biology.

2.2.1 Fluorescent microscopy: its rapid improvement and coupling with other approaches

Fluorescence microscopy presents the key tool for studying cells and biological structures (proteins or organelles) that have been tagged with fluorescent markers (e.g. small organic dyes attached to antibodies directed against proteins of interest, fluorescent semi-conductor quantum dots conjugated to biomolecules or fluorescent proteins as explained thereinafter). In 1873, Ernst Abbe postulated that the smallest distance resolvable in the object plane between two point-like objects cannot be smaller than about half of the light wavelength used for the illumination of the objects. In conventional light microscopy the diffraction barrier limits the imaging resolution to about 200 nm, so that smaller object of interest cannot be resolved. Recently the diffraction limit has been surpassed and the lateral resolution of 20 to 50 nm has been achieved by several novel techniques. These approaches that explore special types of fluorescence microscopes include photoactivated localization microscopy (PALM; Betzig et al., 2006), stochastic optical reconstruction microscopy (STORM; Rust et al., 2006), structured illumination

microscopy (SIM; Gustafsson, 2000) or stimulated emission depletion (STED; Hell, 2003). Some of these microscopes have been already commercialized.

Live cell imaging allows for an investigation of dynamic processes within the cell. This technology is very potent since it usually enables acquiring images with sufficient signal-to-noise ratio without damaging cells. Very fast processes and three-dimensional imaging with multi-labeled samples are often required. Such images can be obtained either by wide-field microscope (WFM) or by the laser scanning confocal microscope (LSCM); for comparison see e.g., Andrews et al. (2002). LSCM scans the sample point-by-point with a light from the laser source and detects emitted fluorescence with a photomultiplier tube (PMT). WFM illuminate the whole sample simultaneously and detect emitted fluorescence with the charge-coupled device camera (CCD camera). The WFM represents an ideal approach for fast imaging of thin objects, such as widely used cells grown in monolayers. In addition, it is also possible to employ an image-processing method called deconvolution to get rid of out of focus light (McNally et al., 1999).

Cells are three-dimensional objects. To generate 3D image requires taking a stack of optical sections. Confocal microscopy offers an advantage over traditional wide-field fluorescence microscopy, because it controls the depth of the field and reduces the out of focal plane signal. In laser scanning confocal microscope, the objective lens collects both in-focus and out-of-focus light, but the confocal pinhole let through only the in-focus light that then reaches the PMT detector. Another approach to deal with blurred (out-of-focus) light is the multiphoton microscope; reviewed e.g., in Diaspro et al. (2006). It limits fluorescence excitation only at the focal point of the microscope. This minimizes the photobleaching and photodamage. Moreover, the long wavelength infrared excitation light (with lower energy than that for classical confocal microscopy) is less harmful to cells.

For live cell experiments, not only the high resolution, but also the speed of image acquisition is important. In such a case the spinning disk confocal microscopy is useful (Nakano, 2002). In this microscope a low dose of multiple excitation beam is applied. As a result, the imaging is accelerated and the photobleaching is decreased.

Fast events on cell surfaces such as vesicle trafficking or endo- and exocytosis can be visualized by total reflection fluorescence microscopy (TIRF) approach (Axelrod et al., 1983). TIRF microscopy utilizes evanescent wave created

by light, which hits the sample in the angle higher than the critical one. At this angle the beam does not pass through the specimen but is totally reflected. The penetration depth of evanescent field is 70-300 nm. Examples of other possibilities how to speed up the imaging and retain confocality are the use of the rapid resonance scanner (produced by Leica) or line scanning mode developed by Zeiss. Based on the character of an experiment, the appropriate imaging technique has to be chosen.

Recent progress in the nuclear organization and function research takes advantage of combination of the state-of-art of fluorescent microscopy with many other approaches. For example, advances in imaging, mass-spectroscopy based proteomics and modern sequencing technologies contributed to the progress in analyzing dynamic events associated with nuclear structure and function, particularly concerning chromatin organization and transcriptional regulation (Trinkle-Mulcahy and Lamond, 2008). Another perspective for cell biology studies consists of a live cell imaging by time-lapse fluorescence microscopy with a subsequent visualization of just observed event of interest under the electron microscope, so called Correlative light and electron microscopy (CLEM). Recently developed automated "Rapid Transfer System" allows fast processing of samples (cryofixation within few seconds followed by cryosubstitution) so that an event observed in live cell by light microscopy can be analyzed at high-resolution in the electron microscope with excellent preservation of ultrastructure (Verkade, 2008).

2.2.2 Fluorescent protein toolbox

The discovery (Shimomura et al., 1962), gene cloning (Prasher et al., 1992) and heterologous expression of green fluorescent protein (GFP; Chalfie et al., 1994) opened possibilities not only for visualization of protein of interest directly in living cells, but also for studying their dynamics over time. Mutagenesis of GFP (Tsien, 1998) and cloning of GFP-like proteins from non-bioluminescent *Anthozoa* species (Shagin et al., 2004) resulted in the wide range of available spectral variants of fluorescent proteins.

DNA sequence that codes a protein of interest is ligated into the expression vector carrying sequence coding a fluorescent protein that is then delivered into cells. The expressed GPF-like fluorescent proteins are unusual since they can form the internal chromophore autocatalytically without requirement of accessory factors but oxygen (Heim et al., 1994).

Desirable attributes of fluorescent proteins include brightness, photostability, rapid maturation, small size, pH insensitivity, tolerance of fusions and resistance to oligomerization. Recently, the new generation of fluorescent proteins capable of changing their optical properties with time or illumination wavelength was introduced. These appropriately termed optical highlighters represent very promising approach for the *in vivo* investigation. Some of these proteins convert from a low (dark) fluorescence state to a bright fluorescence state; this process is termed photoactivation. Other proteins are capable of being optically converted from one fluorescence emission bandwidth to another; this process is known as photoconversion. Moreover, some proteins are capable of reversible photoactivation and quenching. Advantage of these optical highlighters is that we can label a particular protein in a particular area within the live cell. A number of novel techniques were developed using these proteins for cellular studies. Accordingly, one can in time and/or in space monitor highlighted proteins, organelles or cells. Advantage of photoactivatable/photoconvertible protein labeling is that newly synthesized or with time newly folded fusion proteins do not interfere with already highlighted ones. This represents substantial improvement over labeling by photobleaching of "classical" fluorescent proteins, where recovery signals due to newly synthesized proteins need to be taken in an account. Main properties of optical highlighters are listed in the Table 1. An ideal optical highlighters should embody a high level of contrast between activated/photoconverted and non-activated form, and also should be monomeric to be utilizable as a fusion tag.

At the present time, the green-to-red photoconvertible protein Dendra (Gurskaya et al., 2006) appears to be the most promising optical highlighter. Dendra derived from octocoral *Dendronephthya sp*. is monomeric, 26.1 kDa protein. It efficiently matures at 37°C and possesses high photostability of activated form. Dendra photoconversion appears upon 405 nm laser activation, but also 488 nm laser (marginally phototoxic and more widespread in laboratories) was shown to operate for this process. Dendra, as well as all so far reported green-to-red photoconvertible proteins, contains a chromophore derived from the tripeptide His-Tyr-Gly that emits green light. Illumination with UV or violet light induces irreversible cleavage within the chromophore resulting in the red fluorescence of photoconverted species. Improved Dendra2 is commercially available. It comprises a single A224V substitution (outside the chromophore sequence), which leads to its brighter

fluorescence both before and after photoconversion and more complete maturation (Chudakov et al., 2007).

2.2.3 Specific features of *in vivo* imaging of mammalian cells

Mammalian cells need to be cultured under specific conditions and these conditions have to be maintained also during live cell imaging. Simply, cells have to be kept on the microscope stage not only alive but also "happy" since proper conclusions can only be obtained from "healthy" cells. This includes: (i) maintaining temperature at 37°C; (ii) the pH value should be kept within the physiological range which is in most media accomplished by CO_2-$NaHCO_3$ based buffer system requiring 5 % CO_2 atmosphere. An alternative strategy is to add HEPES to medium or to use commercially supplied non-HEPES CO_2-independent medium. (iii) Evaporation of water leads to a harmful increase of the ion concentration. This has to be prevented mainly during long time imaging, for example by sealing the chamber within the microscope setup. (iv) pH indicators such as phenol red are often weakly fluorescent and may present the significant source of noise in live cell experiments. It was also reported (Khodjakov and Rieder, 2006) that phenol red dye could easily photosensitize cells, making them more susceptible to the photodamage during imaging. This problem is easily handled by using commercially available media without pH indicators. (v) Light exposition of the cells should be kept to the possible minimum to avoid/minimize phototoxic effect. (vi) In the cases in which the experimental protocol involving low excitation levels and short exposition times does not sufficiently protect cells, a use of the free radical scavengers (e.g. vitamin C or TroloX) is recommended to reduce the photo-oxidative damage.

3. AIMS OF THE THESIS

The goal of this thesis was to expand our knowledge on the structure-function aspects of the nucleolus and chromatin, particularly nucleolus-associated chromatin, using modern techniques of cell biology, including live cell imaging.

There were two main objectives. First, an important issue regarding maintenance of chromosome organization during cell cycle was addressed. Second, the association of the protein Pontin with the nucleolus was to analyze.

The specific aims are:

- to establish the stable cell line expressing H4-Dendra2 and set-up live cell imaging during which the whole cell cycle can be monitored
- to label specific areas of chromatin by H4-Dendra2 photoconversion and follow the cells by time-lapse through mitosis to the next generation
- to evaluate chromatin labeled pattern in mother and daughter cells, with the focus on the nucleolus-associated chromatin
- to establish the numbers of nucleoli in the daughter cells
- to settle whether the chromatin position is “inherited” in daughter cells
- to establish precisely localization of the protein Pontin within the nucleolus
- to expand the knowledge about the functional significance of this protein in the nucleolus.

4. MATERIAL AND METHODS

A spectrum of molecular and cell biological approaches was employed. These approaches encompassed mainly DNA cloning, cell culturing and synchronization, stable transfected cell line preparation, immunofluorescence, immunoprecipitation, Western blot analysis, siRNA treatment. In addition, the advanced microscopy methods such as photoconversion of fluorescent proteins and live cell imaging were implemented.

As the actual results of my experimental work are presented in the chapters 5 and 6, the detailed description of the materials and methods are provided in each of these chapters separately (subchapters 5.2 and 6.2, respectively).

5. CHROMATIN POSITION IN HUMAN HepG2 CELLS: ALTHOUGH BEING NON-RANDOM, SIGNIFICANTLY CHANGED IN DAUGHTER CELLS

5.1 Introduction

In the post-genomic era, when human genome had been sequenced, we possess a large amount of information about individual genes. However, the function of DNA is not entirely determined by its linear sequence and is, to a large extent, affected by the higher order organization of chromatin fibers and the three-dimensional arrangement of chromosome territotories (CTs)/chromatin (e.g. Fraser and Bickmore, 2007; Misteli, 2007). It has been demonstrated that chromosomes in the interphase nucleus occupy mutually exclusive CTs (e.g. Cremer and Cremer, 2001; Lanctot et al., 2007). A more recent high resolution *in situ* hybridization procedure revealed intermingling of CTs at their borders (Branco and Pombo, 2006). Regardless of their transcriptional activity, genes could be, except some specific cases (Clemson et al., 2006), found anywhere within a CT (e.g. Belmont et al., 1999), and active gene regions were even found to loop out from CTs (Volpi et al., 2000; Williams et al., 2002).

Based on a statistical analysis of large sets of mammalian cells, numerous studies have shown that the CTs are non-randomly arranged within the nuclear space (e.g. Parada and Misteli, 2002). CTs were shown to be preferentially organized radially according to their size and according to their gene density; and even chromosomal bands within a given chromosome were shown to be organized radially according to their density (Boyle et al., 2001; Federico et al., 2008; Kupper et al., 2007; e.g. Parada and Misteli, 2002; Lanctot et al., 2007). It was also reported that CTs have non-random neighborhoods as they occupied preferential positions relative to one another (Nagele et al., 1999 - however, see Bolzer et al., 2005; Parada et al., 2003; e.g. Parada and Misteli, 2002). Several contacts between different chromosomal loci were reported, which may contribute to gene silencing or activation (e.g. Cavalli, 2007; Meaburn et al., 2007).

Several reports showed that the CT/chromatin order is, within nuclei, to a large extent stably maintained during interphase in cultured mammalian cells, except the early G1 phase of the cell cycle during which some increased chromatin mobility was observed (Gerlich et al., 2003; Walter et al., 2003; Thomson et al., 2004;

Wiesmeijer et al., 2008). At the same time, it is to be emphasized that, during development, differentiation or upon experimental modulation of cell metabolism, not only smaller, but even extensive changes of CT/chromatin or chromatin domains nuclear position are observed (e.g. Chuang and Belmont, 2007; Kumaran et al., 2008); it should be noted, however, that some data discussed in the review by Kumaran et al. (2008) have been retracted meanwhile (Nunez et al., 2008a; Nunez et al., 2008b) .

The non-random organization of chromosomes in mammalian nuclei raises a question: Is, or is not, the CT/chromatin position, together with its neighbourhood, preserved through mitosis in daughter cells? This question has already been addressed with divergent results obtained (Berr and Schubert, 2007; Essers et al., 2005; Gerlich et al., 2003; Thomson et al., 2004; Walter et al., 2003; e.g. Bickmore and Chubb, 2003; Gerlich and Ellenberg, 2003; Parada et al., 2003; Williams and Fisher, 2003). It should be noted that the prototype studies by Gerlich et al. (2003), Walter et al. (2003) and Essers et al. (2005) claiming either preservation of chromatin position or its significant positional changes in daughter cells, were performed on selected nuclear chromatin regions - in the form of the nuclear pole, the sector of nucleus and the half of nucleus - of unknown content and function.

In this respect, the cell nucleus contains many structures/bodies such as nucleolus, Cajal bodies and PML (promyelocytic leukemia) bodies that are linked with a particular nuclear function, and often associate with distinct chromosomal sites (Frey et al., 1999; Schul et al., 1999; e.g. Parada and Misteli, 2002). The best characterized example of nuclear bodies-chromosomal loci associations is the nucleolus (e.g. Boisvert et al., 2007; Raška et al., 2006a). Beside other functions, the nucleolus is the structure in which rRNA is synthesized and ribosome biogenesis takes place. Ribosomal genes are arranged in arrays of head-to-tail tandem repeats called nucleolus organizing regions (NORs), which are in human cells located within the short arms of 5 acrocentric chromosomes 13, 14, 15, 21 and 22. Human cell nuclei typically contain one to several nucleoli. At the onset of mitosis ribosomal genes cease to transcribe and nucleoli disintegrate. rRNA synthesis resumes at the end of mitosis, ribosomal arrays from more than one NOR-bearing chromosome (NOR-chromosome) then often cluster, and respective nucleolus is reformed around them. Reformation of the nucleolus in early G1 phase thus proceeds through interactions between different CTs, and the nucleolus-associated chromatin (NAC)

corresponds significantly, but not exclusively, to parts of NOR-chromosomes with ribosomal genes being rather engulfed within nucleoli (Kalmárová et al., 2007; Leger et al., 1994; Manuelidis and Borden, 1988; Smirnov et al., 2006). In the electron microscopic image, a rim of heterochromatin typically surrounds nucleoli as the result. An investigation whether the NAC position is, or is not, preserved across mitosis would then have higher relevance than that of chromatin regions of completely unknown content and function.

It should be noted that the exact molecular mechanism for the existence/maintenance of nucleoli is still to be established. The involvement of NORs and transcription of ribosomal genes represent indeed a key condition (e.g. Raška et al., 2006a). However, it is not a sufficient condition due to the presence of numerous protein and RNA molecule factors affecting the nucleolar function/structure (Gonda et al., 2003; Peng and Karpen, 2007 and references there in).

In this work, we re-investigated the behavior of previously described chromatin regions of unknown composition and investigated the behavior of NAC through mitosis up to the next interphase in daughter cells. We took advantage of newly developed green to red photoconvertible protein Dendra2 (Gurskaya et al., 2006) that allowed us, via fusion protein histone H4-Dendra2, to selectively label different chromatin regions in transfected human HepG2 (HepG2$^{H4\text{-}Dendra2}$) cells, monitor by time-lapse imaging large number of cells and apply quantitative analysis of labeled chromatin distribution in mother and daughter cells.

5.2 **Materials and Methods**

5.2.1 **H4-Dendra2 construct and HepG2 $^{H4\text{-}Dendra2}$ stable cell line**

H4-Dendra2 was generated from full-length of human histone H4 (from pBOS H4-N-GFP expression vector, kind gift from H. Kimura), which was flanked by PCR with XhoI and EcoRI restriction sites and ligated into those sites of pDendra2-N (Evrogen).

The construct was transfected into uneuploid HepG2 cells using Effectene (Qiagen) and stable clones were selected with G418. One clone with bright Dendra2 fluorescence was chosen and expanded into the cell line. HepG2$^{H4\text{-}Dendra2}$ stable cell line was cultured in Dulbecco's modified Eagle's medium with 10 % fetal bovine serum, supplemented with penicillin-streptomycin, but without G418. For

microscopy, cells were cultured in glass bottom Petri dishes (MatTek). Live cell imaging was performed in phenol red-free medium.

Besides it, in order to evaluate nucleolar counts, HepG2, HepG2$^{H4\text{-}Dendra2}$, HeLa (Kalmárová et al., 2008) and human primary LEP fibroblast (Sevapharma) cells were cultured under standard conditions.

5.2.2 **Dendra2 photoconversion and live cell imaging**

Live cell imaging was performed with Leica TCS SP5 accessorized with large size temperature incubator with CO_2 controller (Life Imaging Services) and using 63x/1.4 NA oil immersion objective.

Non-activated Dendra2 exhibited green fluorescence visualized with 488 nm Ar laser. To label specific chromatin region, Dendra2 was activated with 405 nm diode laser line. Photoconverted Dendra2 exhibited a bright red fluorescence (visualized with 561 nm DPSS laser line), while the green fluorescence was partially bleached. It should be noted that we tried in vain to activate Dendra2 with accessible Leica TCS SP2 equipped with 2-photon excitation.

For time-lapse experiments, cells were partially synchronized by incubation with 3 mM thymidine (Sigma) for 16 hours. The same experiments were also performed with non-synchronized cells and, although a lower number of cells could be analyzed, entirely compatible results on labeled chromatin were obtained (Z. Cvačková, unpublished).

Time-lapse was mostly set to 30 min intervals and by sequential scanning of green and red fluorescence of H4-Dendra2 was visualized overall chromatin and chromatin marked by photoconversion, respectively. At low power of 488 nm laser used, such repeated scanning of green fluorescence did not lead to any observable Dendra2 activation if performed in control experiments, in which Dendra2 conversion was omitted (Z. Cvačková, unpublished). Bright field was also captured to control the morphology of cells. Time-lapse imaging was run overnight. Prolonged time-lapse imaging until the third interphase was also performed.

More than 500 cells were evaluated in time-lapse experiments in total and a special care was paid to the deleterious phototoxic effect. In order to limit its extent, we restricted the acquisition of 3D scans in most experiments to the initial moment just after photoconversion and to the final moment at the end of the time-lapse experiment.

5.2.3 **Western blot analysis**

Whole-cell lysates were separated on 12 % SDS-PAGE and transferred to nitrocellulose membranes (Protran). The membranes were incubated with rabbit anti-histone H4 (Abcam) or rabbit anti-Dendra (Evrogen) and then goat anti-rabbit secondary antibodies conjugated with horseradish peroxidase (Jackson) in a standard way. Horseradish peroxidase activity was detected using an ECL chemiluminiscence system (Pierce) and captured with X-ray film (Foma).

5.2.4 **Length of the cell cycle**

Doubling time of unsynchronized cultured cells was 18.68±2.24 hours. To ensure that the beginning of the time-lapse experiments with partially synchronized cells was set several hours prior mitosis and the end at least 4 hours after mitosis, relative ratio of cell cycle phases (G1, S and G2 together with mitosis) was in unsynchronized cells established using flow cytometry of propidium iodide labeled cells (Beckman Coulter, Cell Lab Quanta); in addition, S phase length was evaluated on the basis of the immunocytochemistry of incorporated 5-bromo-2-deoxyuridine (Sigma) (Z. Cvačková and M. Mašata, unpublished).

5.2.5 **Image processing and data evaluation of labeled chromatin regions of unknown composition**

To quantitatively analyse the nuclear distribution (degree of compactness) of labeled chromatin (the nuclear pole, the segment of nucleus and the half of nucleus) in the mother and the daughter cell nuclei, averaged distance (pixels of 60 nm) of photoconverted signal from the gravity centre of this signal was measured. In the case of identical distribution there should be similar averaged distances in the mother and the daughter cells. To compare these distances to the situation mimicking a random distribution of chromosomes in nuclei, we also calculated these average distances over whole nuclei. For clearness, the real averaged distance is given as the percentage of the random distribution distance.

All evaluations were done on thresholded (binary) images. As the choice of correct threshold is highly subjective, it was performed manually only for photoconverted signal in mother cells in which the treshold values were easy to determine (in Photoshop). For daughter cells, the threshold was calculated

automatically under condition that there was the same amount of activated pixels as in mother cells (in Matlab). It should be noted that the calculated averaged distances were not sensitive to small variation in the threshold setup.

5.2.6 **Fluorescent *in situ* hybridization of chromosomes and number of nucleoli**

The immunocytochemical visualization of nucleoli via fibrillarin mapping and the *in situ* hybridization of all NOR-chromosomes 13, 14, 15, 21 and 22, as well as of chromosomes 6, 10 and 18, was performed as in Kalmárová et al. (2007).

To compare numbers of nucleoli in the two daughter cells, the mitotic cells were seeded, processed 4 hours after seeding for the immunocytochemical visualization of nucleoli, and nucleolar counts in 100 pairs of daughter cells were evaluated. In 4 experiments, only 19, 20, 24 and 24 % pairs exhibited the same number of nucleoli, and the values 22.0, 21.4, 22.0 and 21.8 % of the corresponding random pairing model (Kalmárová et al., 2008) fitted well these counts. Furthermore, the incidence of the same number of nucleoli in the three cells (i.e. the mother cell and the two daughter cells) was in time-lapse experiments with partially synchronized cells ranging between 3 and 7 %. Results of nucleolar counts in daughter cells, performed in the same way with HeLa cells and non-transfected HepG2 cells (Kalmárová et al., 2008; E. Smirnov and M. Kalmárová, unpublished), matched perfectly those observed in HepG2$^{H4\text{-}Dendra2}$ cells. In addition, analogous experiments with human primary LEP fibroblasts exhibiting lower number of nucleoli (mean number 2.78 nucleoli versus 3.63 value observed in HepG2$^{H4\text{-}Dendra2}$ cells) showed that more than 67 % of pairs of daughter cells exhibited different nucleoli numbers.

5.2.7 **Image processing and data evaluation of the nucleolus associated chromatin**

Best focus light-optical sections were further processed. First, the areas of the nucleoli and the nucleus were manually defined in RGB channels in Photoshop CS software according to bright field and H4-Dendra2 signal, respectively. Then, employing a routine written in MatLab software, each cell was divided into 15 equivalent regions, concentrically arranged around all nucleoli within the nucleus (Fig. 5.4). Intensity of the red fluorescence was averaged within every region and plotted against the distance of this region from the nucleoli borders. Since the signal

of converted H4-Dendra2 was split from the mother cell into the two daughter cells, the daughter cell curve was normalized (same area under the curve as in the mother cell curve) to enable direct comparability between both curves.

Specially with respect to the experiments with the NAC, we were aware of the deleterious effect due to the illumination cone and evaluated the extent of the 3D activation "noise". We found it, in contrast to experiments in which the half of nucleus and the nuclear segment were labeled, of limited importance particularly with larger nucleoli (Fig. 5.1D). To minimize this effect, time-lapse experiments of NAC were quantitatively evaluated under condition that mother cell was mainly bearing larger nucleoli.

5.3 **Results**

5.3.1 **Characterization of the HepG2 cells expressing photoconvertible histone H4-Dendra2**

To address chromatin behavior, we first established a stable cell line carrying histone H4 tagged with the photoconvertible protein Dendra2 that was connected to the C-terminus of the histone H4 through a linker of 17 amino acid residues. This cloning strategy enabled the N-terminus of histone to be accessible for post-translation modifications (Kimura and Cook, 2001) and a linker facilitated incorporation of the fusion H4-Dendra2 protein into the nucleosome. Photoconvertible fluorescent protein Dendra2 tagged to H4 allows to label and follow selected chromatin regions (red fluorescence of converted Dendra2) and, at the same time, to monitor the whole chromatin (green fluorescence of non-converted Dendra2) in living cells (Fig. 5.1A). In addition, it was shown (Kimura and Cook, 2001) that the inner core histones H3 and H4 are less exchanged in the nucleosomes as compared to the outer histones H2A and H2B, and thus represent better markers for long-term observation than H2B histone used in previous studies (Essers et al., 2005; Gerlich et al., 2003; Walter et al., 2003).

HepG2 cells were chosen because generally cancer cells, that allow for the establishment of stable transfection, are less sensitive to photodamage than primary cells and therefore more suitable for long-term live cell imaging experiments (Walter et al., 2003). After Dendra2 photoconversion, 87 % of cells (out of more than 500 analysed cells) passed through mitosis without morphological abnormalities or delay in the cell cycle, which indicated that the laser pulse used for the photoconversion

(and image acquisitions) did not cause major defects. Moreover, photoconverted cells passed also the second mitosis during prolonged live cell imaging. However, the signal of activated Dendra2 in granddaughter cells was too weak and did not allow further evaluation (Z. Cvačková, unpublished).

5.3.2 **Chromatin position is rather stable during interphase but, although being still non-random, is significantly changed in a vast majority of daughter cells**

To test chromatin behavior during interphase and mitosis, the randomly chosen chromatin regions of two regular shapes with distinct topologies, rings and crosses, were labeled within nuclei by H4-Dendra2 photoconversion and the cells were observed by time-lapse imaging (Fig. 5.1B-D). Cells were partially synchronized to G1/S phase boundary by one thymidine block, labeling was performed shortly after release from the block and the time-lapse was run overnight. During this time the red signal of converted Dendra2 remained detectable. The regions of labeled chromatin exhibited only minor changes from the moment of photoconversion until mitosis onset, and the labeled rings and crosses remained clearly distinguishable. During mitosis and early G1 phase, labeled regions of chromatin were rearranged. The pattern of labeled chromatin formed in later G1 phase typically largely differed from regular shapes labeled in the previous cell cycle. However, similarly to the situation encountered in the previous cell cycle, this pattern of labeled chromatin was rather stable, exhibiting just minor changes until the end of time-lapse (Fig. 5.1B,C).

To further evaluate a general chromatin position during the cell cycle we expanded our study and randomly labeled, approximately 4 hours after release from the block, three different regions of the nuclear chromatin as in previously published studies: the nuclear pole, the sector of nucleus and the half of nucleus (Essers et al., 2005; Gerlich et al., 2003; Walter et al., 2003). The distribution of the labeled chromatin in the daughter cells was different in a vast majority of daughter cells; it did not achieve the mother cell-like compact shape and the signal of converted H4-Dendra2 was scattered in most cells (Figs. 5.2, 5.3A,B). Cells showing a labeled pattern, that to some extent resembled the situation in mother cells, were not frequent and their occurrence in individual live cell imaging experiments ranged between 0 % and 25 %.

We have to emphasize that the major drawback in this kind of experiments is to be attributed to the unknown chromatin composition of the labeled region. Accordingly, within the frame of one single live cell imaging experiment, the labeled chromatin regions in different mother cells had different composition. And even if the pattern of the label seen in the daughter cells resembled to some extent to that seen in the mother cell, we can hardly say anything about the chromatin/CT order preservation within the labeled region, except if some additional markers apply such as nucleoli (Fig. 5.3B).

This being said, the quantitative evaluation of data with labeled regions of unknown composition showed that the distribution of signal in the daughter cells was not identical with that in the mother cell but is not, at the same time, scattered randomly as values in the daughter cells neither approached the values seen in mother cells, nor reached value 100 % (Fig. 5.3A). In fact, whatever was the selected chromatin region, the average distribution of label in daughter cells corresponded to the distribution being roughly in a midway between identical and random distribution (Fig. 5.3A), i.e. the distribution was non-random. It could be also seen that the calculations are mainly sensitive for small activated regions (the nuclear pole) while there was not enough space for chromosomes to move if a large region was activated (the half of nucleus); the sector region experiments provided intermediate results. With respect to the value of significance ascribed to experiments with photoconverted chromatin regions of unknown composition, the choice of the nuclear pole region is to be considered as by far the best choice since the photoconversion affected at most several chromosomes only. The results of live cell imaging experiments with the nuclear pole region provided straightforward images of scattered labeled chromatin (Fig.5.2, 5.3A), and necessarily argued against the preservation of chromatin position, at its large scale organization, in most cells.

An important issue also concerns the number of (fully or partially) labeled CTs within the labeled region. As already mentioned, the nuclear pole region is the best choice as only several CTs were labeled at most while numerous CTs were labeled in the sector of nucleus and the half of nucleus nuclear regions. In order to minimize the number of labeled CTs, we photoconverted the smallest possible region in the nuclear periphery affecting just a very few CTs under condition that the signal could be still evaluated in the daughter cells. We observed that the distribution of signal in many cells, but not in all daughter cells, was scattered into two or more

labeled regions and thus largely differed from that seen in the mother cell (Fig. 5.3C).

The results obtained with labeled chromatin regions of unknown composition in HepG2$^{H4\text{-}Dendra2}$ cells showed that the chromatin position is from the time of photoconversion to the onset of mitosis as well as from the later G1 phase until the end of live cell experiment rather stable, displaying only minor changes. Extensive changes in the distribution of the chromatin signal are observed after mitosis in most daughter cells, but the chromatin position still has non-random character.

5.3.3 **Different nucleoli numbers are incompatible with the preservation of CT/chromatin position in daughter cells**

The inconvenience of above mentioned experiments was completely unknown composition of labeled chromatin regions. In order to circumvent this problem, at least to some extent, we turned to the NAC as it is known that a significant part of it contains DNA sequences belonging to NOR-chromosomes. Accordingly, we first established the association of various chromosomes with nucleoli via combined mapping of relevant chromosomes by fluorescence *in situ* hybridization (FISH) and nucleoli by immunocytochemistry. We also evaluated the number of nucleoli in nuclei of HepG2$^{H4\text{-}Dendra2}$ cells.

In agreement with our previous studies with human HeLa cells and primary human fibroblasts (Kalmárová et al., 2007, 2008; Smirnov et al., 2006), human NOR-chromosomes (chromosomes 13, 14, 15, 21 and 22) exhibited frequent associations with nucleoli of HepG2$^{H4\text{-}Dendra2}$ cells, with FISH signal penetrating sometimes within nucleoli. We also performed FISH with chromosomes 6, 10 and 18 and observed some associations of these chromosomes with nucleoli, but the frequency of associations was considerably less than that with the NOR-chromosomes (Z. Cvačková, unpublished results).

HepG2$^{H4\text{-}Dendra2}$ cells exhibit usually one to five nucleoli. The counting of nucleoli revealed significant differences between the two daughter cells as also shown in parallel experiments with HeLa cells by Kalmárová et al. (2008) and non-transfected HepG2 cells (see Materials and Methods). Only less than 25 % of daughter HepG2$^{H4\text{-}Dendra2}$ cell pairs (see Materials and methods) exhibited the same numbers of nucleoli. This finding demonstrated that nuclear positioning of at least all chromatin NOR domains was not identical in more than 75 % pairs of daughter cells.

As nucleoli were in nuclei usually found separated by several micrometers, our results also indicated that different sets of NOR-chromosomes differently associated with individual nucleoli in a majority daughter cells, this finding being incompatible with the chromatin position preservation in the daughter cells.

Importantly in this respect, different numbers of nucleoli were also present in a majority of daughter cell pairs of primary human fibroblasts (see Materials and Methods). More than 67 % pairs of daughter cells exhibited different numbers of nucleoli. This percentage was lower than that in transformed investigated cells but it should be noted that the average number of nucleoli within nuclei of primary cells was also lower (see Materials and Methods).

In summary, our results with HepG2$^{H4\text{-}Dendra2}$ cells are in agreement with the established fact that a significant part of the NAC corresponds to chromatin of NOR-chromosomes. Our results demonstrating the differences in nucleolar counts are not in harmony with the preserved CTs/chromatin position in a majority of daughter cells.

5.3.4 **The NAC is dispersed in daughter cells and differently associates with different nucleoli**

To verify the conclusions arising from nucleolar countings also in living cells as well as to investigate behavior of chromatin region, the significant part of which is composed of parts of NOR-chromosomes, we selectively labeled the NAC in mother cells and followed the fate of labeled chromatin up to the next interphase in the daughter cells.

A ring of chromatin was labeled by photoconversion of H4-Dendra2 at the closest vicinity of nucleoli that were revealed by bright field imaging (Fig. 5.4). The extent of labeling due to the contribution of the illumination cone was found to be of a limited importance (Fig. 5.4D). Cells were partially synchronized by one thymidine pulse and released from the block approximately 4 hours prior to photoconversion. Thus, majority of cells were in S or G2 phase as also confirmed by immunocytochemistry of incorporated 5-bromo-2-deoxyuridine (Z. Cvačková and M. Mašata, unpublished). The ring-shaped pattern of labeled chromatin remained well distinguishable until mitosis onset, although a minor chromatin movement/histone exchange could be seen. Distribution of labeled chromatin in daughter cells was seen in high-resolution images that were taken several hours after

mitosis (Fig. 5.4A). At that time, the daughter cells were passing through later G1 or even later interphase, i.e. the period when the chromatin pattern was expected to become rather stable; indeed, the labeled pattern in daughter cells remained rather stable, exhibiting just minor changes, from later G1 until the end of time-lapse imaging. However, the pattern was dispersed and largely differed from the mother cell-labeled pattern in all monitored cells (Fig. 5.4A,C; Movie 5.1), this being not in harmony with a concept of the chromatin position preservation.

The video (30 min snapshot intervals) showing the behavior of the labeled NAC in the mother and the daughter cells encompassed 15 hours. Note that only partially synchronized cells were used and one mother cell was labeled at the onset of mitosis. This resulted in a special distribution of the signal in the respective daughter cells due to the already reorganized chromosomes in the mother cell.

Fluorescent images of converted and overall non-converted H4-Dendra2 chromatin together with the bright field snapshots were recorded several hours before, and several hours after, cell division (Fig. 5.4), and the position of labeled chromatin with respect to all the nucleoli in the given nucleus was quantitatively evaluated (Fig. 5.4E-G) as described in Materials and Methods. To analyse data more accurately, we also took into account a contribution of chromatin movement/histone H4-Dendra2 exchange during the live cell imaging. There were a few cells that failed to divide in the course of the whole time-lapse (Fig. 5.4B), which were used to determine the extent of chromatin movement/histone H4-Dendra2 exchange. Although only 2D quantitative evaluation of the signal was performed, the character of curves shown in Fig. 5.4E was clear-cut. Juxtaposition of labeled chromatin in these cells with distribution of labeled chromatin areas in daughter cells revealed that, even though being differently dispersed, approximately 70 % of labeled chromatin located to the closest vicinity of different nucleoli in the daughter cells. Similar results, with labeled chromatin being located to the vicinity of different nucleoli in the daughter cells, were obtained if the NAC of just one out of several nucleoli present in the nucleus was labeled in the mother cell (Z. Cvačková, unpublished).

As a control, rings of similar size were labeled in "randomly" chosen chromatin region non-containing nucleoli. Acquired snapshots were subsequently processed as in the above experiments (Fig. 5.4F). The labeled pattern formed in

daughter cells largely differed from original one (Z. Cvačková, unpublished) but exhibited no bias for the nucleolar vicinity.

Our live cell experiments thus showed that much of the mother HepG2$^{H4\text{-}Dendra2}$ cell-labeled NAC signal is still associated with nucleoli in the daughter cell nuclei, this reflecting implicitely the well established fact that functional NOR domains cluster in the nucleus and NOR-chromosomes are associated with nucleoli. However, the signal has a dispersed pattern and is differently associated with different daughter cell nucleoli.

5.4 **Discussion**

The "inheritance" of chromosome order in the mammalian daughter cells (Gerlich et al., 2003) is without any doubt a very strong claim not only within the context of biology of the cell, but also human medicine (Roix et al., 2003; e.g. Meaburn et al., 2007). Most importantly, the last publication directly relevant to the present study (Essers et al., 2005) strengthens the claim of "inheritance" of chromosome order. Accordingly, the aim of the present study was to reconcile the previously published divergent results and, with the NAC experiments, to expand the information concerning the question "Is, or is not, the CT/chromatin position, together with its neighbourhood, preserved through mitosis in daughter cells?"

Results of numerous FISH experiments led to a consensus that chromosomes are arranged in mammalian nuclei non-randomly in cell/tissue specific manner (Parada et al., 2004; e.g. Lanctot et al., 2007). We emphasize that this consensus for the non-random arrangement is based on statistical evaluations of hundreds of cells, but does not necessarily apply to individual investigated cells. Algorithm, through which the 3D non-random organization of chromosomes is achieved, is as yet unknown.

The GFP technologies allowed, by time-lapse imaging of living cells, to test whether the nuclear arrangement of CTs/chromatin in the daughter cells is preserved with respect to that in the mother cell. In contrast to previous studies in which recombinant H2B-GFP protein was used (Essers et al., 2005; Gerlich et al., 2003; Walter et al., 2003), we used here H4 histone that is known to be less exchanged than H2B histone (Kimura and Cook, 2001) and, via photoconversion, we also avoided the problem of newly synthesized recombinant proteins used in bleach-labeled experiments performed previously. We also paid attention to the exclusion of cells

just entering mitosis during photoconversion (Movie 5.1), this fact, in our opinion, possibly representing one reason leading to divergent results previously published in the literature

We were careful concerning the deleterious effect of phototoxicity and we rather relied on the live cell experiments during which the 3D pictures were taken just at the beginning and at the end of the time-lapse experiments, instead those in which the 3D images were acquired throughout the whole duration of the experiment. Although all the cells were necessarily affected by the light, almost 90 % of monitored cells exhibited convenient biological behavior.

Whatever was the kind of labeled chromatin region, the distribution of label did not show major changes during the investigated periods of the cell cycle from the moment of photoconversion until mitosis onset as well as from the later G1 phase of the consecutive interphase until the end of the time-lapse experiment, this result being in agreement with the findings of previous studies (Gerlich et al., 2003; Thomson et al., 2004; Walter et al., 2003; Wiesmeijer et al., 2008).

Our results from numerous live cell imaging experiments with the labeled regions of unknown composition are not consistent with a concept of the preservation of CT/chromatin position in mammalian daughter cells (Essers et al., 2005; Gerlich et al., 2003). In contrast, they are in agreement with findings reported by Walter et al. (2003), according to which significant changes of chromatin position after mitosis and early G1 were established. It was already discussed that the published contradictory results could be caused by using different cell type, cells from different species or different timing of bleach-labeling of mother cells within the cell cycle (Bickmore and Chubb, 2003). We repeated in the present study the relevant experiments that were previously described in the literature and in which divergent conclusions were reached. Importantly, the re-visited divergent issue in the present study provided entirely consistent results showing that chromatin position seen in the mother cell is extensively changed in most HepG2$^{H4\text{-}Dendra2}$ daughter cells while still exhibiting non-random character (Fig. 5.3A).

We emphasize that the used methodical strategy investigating the behavior of randomly selected chromatin region of unknown composition can only be used for the proof or the disproof of the identical CTs/chromatin positioning in mother and daughter cell nuclei, and for nothing between. Just one demonstration of different distribution of the labeled chromatin in mother and daughter cell nuclei is

theoretically sufficient for the disproof of identical nuclear CTs/chromatin arrangement. On the contrary, any randomly chosen photoconverted chromatin region of any pattern should not be omitted from the labeling and subsequent analysis of its distribution in mother and daughter cell nuclei for the proof of identical, i.e. "inherited", nuclear CTs/chromatin arrangement. In our experiments, some daughter cells exhibited (to some extent) similar distribution of labeled chromatin as seen in the mother cell. But this may rather reflect the lucky random labeling of chromatin region in the mother cell, the particular chromatin domains of which fulfill some of the (unknown) rules of the non-random 3D organization (like e.g. always together at the nuclear periphery). But even if so, we have hardly any control of what happened within the labeled region (regions) seen in the daughter cells (see however Fig. 5.3B).

The conclusion about the significantly different arrangements of CTs/chromatin of unknown composition in daughter cells was also reached with a help of immunocytochemistry that revealed different numbers of nucleoli in most investigated cells. This finding demonstrated that the 3D arrangement of NOR-chromosomes cannot be preserved in a majority of daughter HepG2$^{H4\text{-}Dendra2}$ cells as well as HeLa cells (Kalmárová et al., 2008), non-tranfected HepG2 cells and primary human LEP fibroblasts. At the same time, importantly, Kalmárová et al. (2008) reported that although the daughter HeLa cell pairs typically had different numbers of nucleoli, the associations of NOR-chromosomes 14, as well as NOR-chromosomes 15, with nucleoli in the two daughter cells were non-random. This indicated that the distribution of the NOR-chromosomes among the nucleoli is partly conserved through mitosis.

The investigation of the behaviour of photoconverted NAC, the significant part of which consists of NOR-chromosomes, across mitosis is more relevant than that concerning chromatin regions of unknown content and function. In agreement with these results, our time-lapse imaging results documenting the behavior of all labeled NACs (as well as the NAC of just one out of several nucleoli present in the nucleus being labeled) in the mother cell nucleus showed that the distribution of labeled chromatin in all monitored daughter cells was dispersed and differed from that originally labeled in the respective mother cell. Even though possibly exhibiting non-random features (Kalmárová et al., 2008), the mother cell-labeled NAC differently associated with different daughter cell nucleoli. This represented also the

first indirect visualization and support of combinatory variability of NOR clustering during post-mitotic *de novo* formation of nucleoli in living cells, hitherto suggested by statistical evaluation of immunocytochemical/FISH results only.

Our results concerning both various labeled chromatin regions of unknown composition and labeled NAC, are, importantly, not contradictory to the non-random 3D organization of chromosomes (Fig. 5.3A). They rather reflect the elementary fact that non-random does not necessarily mean identical. The accepted non-random 3D nuclear organization of chromosomes is compatible with more than one spatial arrangement of functionally specific chromatin domains (like NORs), chromosomes (like NOR-chromosomes) and functional nuclear subcompartments (like nucleoli; different numbers of nucleoli and nucleoli differently located in the nucleus).

The algorithm of non-random, cell/tissue-specific 3D nuclear arrangement of mammalian chromosomes (Parada et al., 2004; e.g. Lanctot et al., 2007) apparently allows more than one arrangement, i.e. it possesses multiple degrees of freedom. Accordingly, a possibility exists that the rare, identical CTs/chromatin arrangement might be achieved after mitosis; however, the evidence of identity requires incomparably more data than the evidence of non-identity with the methods and strategy currently used in this type of live cell imaging.

Our data on mammalian chromatin position fit the model of nuclear self-organization (e.g. Kurakin, 2007; Misteli, 2007), with chromatin being highly dynamic and its structure-function organization encompassing, importantly, also stochastic as well as "plasticity" (adaptive) features. It is an implicit model in which the sum of all properties of a chromosome determines its position (Misteli, 2007); but still, all this is a subject to stochasticity and adaptivity, and the relevant explicite molecular mechanisms remain to be established. Even a much more straightforward task - the exact determination of molecular mechanisms that stand behind the existence/maintenance of nucleoli - is not yet settled. In terms of CTs/chromatin non-random positions, it is governed via an unknown algorithm exhibiting multiple degrees of freedom, i.e. stochastic features. We are of the opinion that the cells are confronted with multiple possibilities how the nucleus is to be reassembled, with the arrangement of CTs/chromatin becoming rather stable later on during the G1 phase of the consecutive interphase.

Our results support the findings of Walter et al. (2003) and Thomson et al. (2004) who did not claim "inheritance", but *de novo* establishment of the

CTs/chromatin positioning in daughter cells during early G1 phase, such a positioning encompassing a significant stochastic component. In this respect, (Kumaran and Spector, 2008) showed that the cell necessitates to go through mitosis for an appropriate localizations of the investigated genetic locus to the peripheral nuclear lamina and proposed that the contribution by the lamina in establishing nuclear architecture and chromatin organization occurs during the early G1 phase.

Coming back to the results on chromatin regions of unknown composition in HepG2$^{H4\text{-}Dendra2}$ cells, chromosomes are inherited in daughter cells, but CTs/chromatin positioning is not "inherited", although it still complies to the rules of the non-random positioning. Specifically speaking about nucleoli, nucleoli disintegrate during mitosis, but NOR-chromosomes are inherited. Functional NOR domains from several NOR-chromosomes then cluster within the nucleus and much of the originally labeled NAC is found associated with nucleoli in the daughter cells. However, NOR-chromosomes cluster in different and variable combinations, and give rise to different numbers of nucleoli in the daughter cells. Based also on our previous results with HeLa cells (Kalmárová et al., 2008), we infer that all those chromatin rearrangements in HepG2$^{H4\text{-}Dendra2}$ comply to the non-random nuclear 3D organization of NOR-chromosomes.

Taken together, the results of the present study support the view that chromatin position is significantly rearranged in a vast majority of HepG2$^{H4\text{-}Dendra2}$ daughter cells, while still complying to the non-random CTs/chromatin arrangement, i.e. the CTs/chromatin arrangement being partly preserved.

5.5 **Figures**

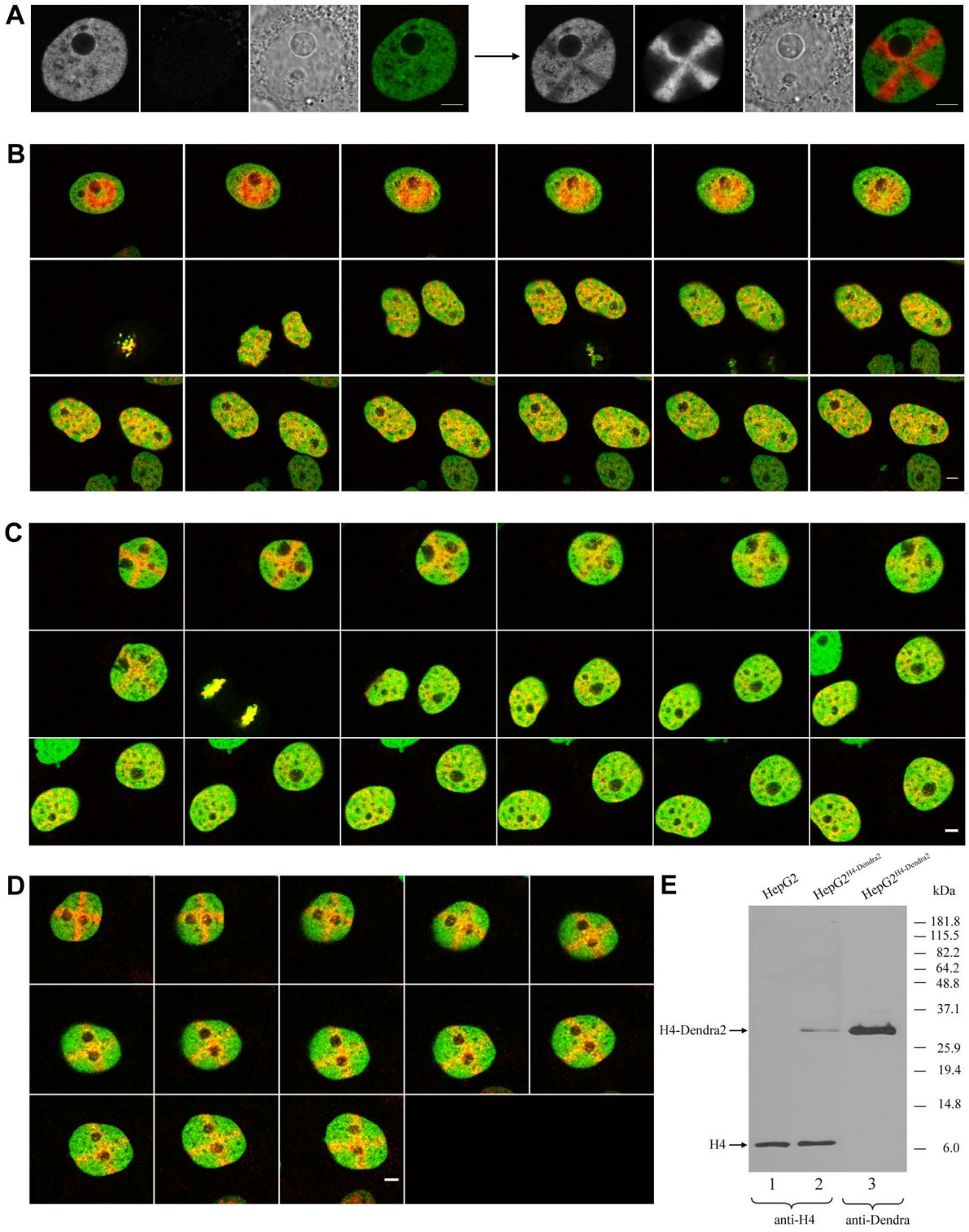

Figure 5.1 Characterization of HepG2$^{H4\text{-}Dendra2}$ stable cell line and chromatin behavior during interphase and mitosis recorded by time-lapse imaging. **(A)** Non-activated Dendra2 exhibits green fluorescence. Activation results in bright red fluorescence, while the green fluorescence is partially bleached. The two channels,

phase contrast and merged signals are shown. Scale bars: 5µm. **(B-D)** Shortly after release from the thymidine block, regular shapes, rings (in Fig. B) and crosses (in Fig. C,D), are highlighted in chromatin by Dendra2 photoconversion and the behavior of labeled chromatin is followed across the mitosis. Individual pictures are shown in one hour intervals. Scale bars: 5µm. In Fig. B,C, the labeling pattern exhibits some chromatin movement and/or histone exchange, but the pattern of rings and crosses remains well distinguishable from the moment of activation until the onset of mitosis. The chromatin pattern formed in later G1 differs significantly from the regular shapes labeled in the foregoing cycle, but remains again to a large extent unchanged until the end of the time-lapse imaging. In Fig. D, an example of the labeled cell, which fails to divide during a course of 12 hours, is given. Note rotation of the nucleus in this Figure as well as in Fig. 4C. **(E)** Western blot analysis of whole cell lysates of untransfected and stably transfected HepG2 cells. Equivalent amount of proteins were loaded and incubated with anti-H4 (lines 1 and 2) or anti-Dendra antibodies (line 3). Bands corresponding to the endogenous and Dendra2-tagged histones are designated. With respect to H4-Dendra, the relative amount of small endogenous H4 may be underestimated.

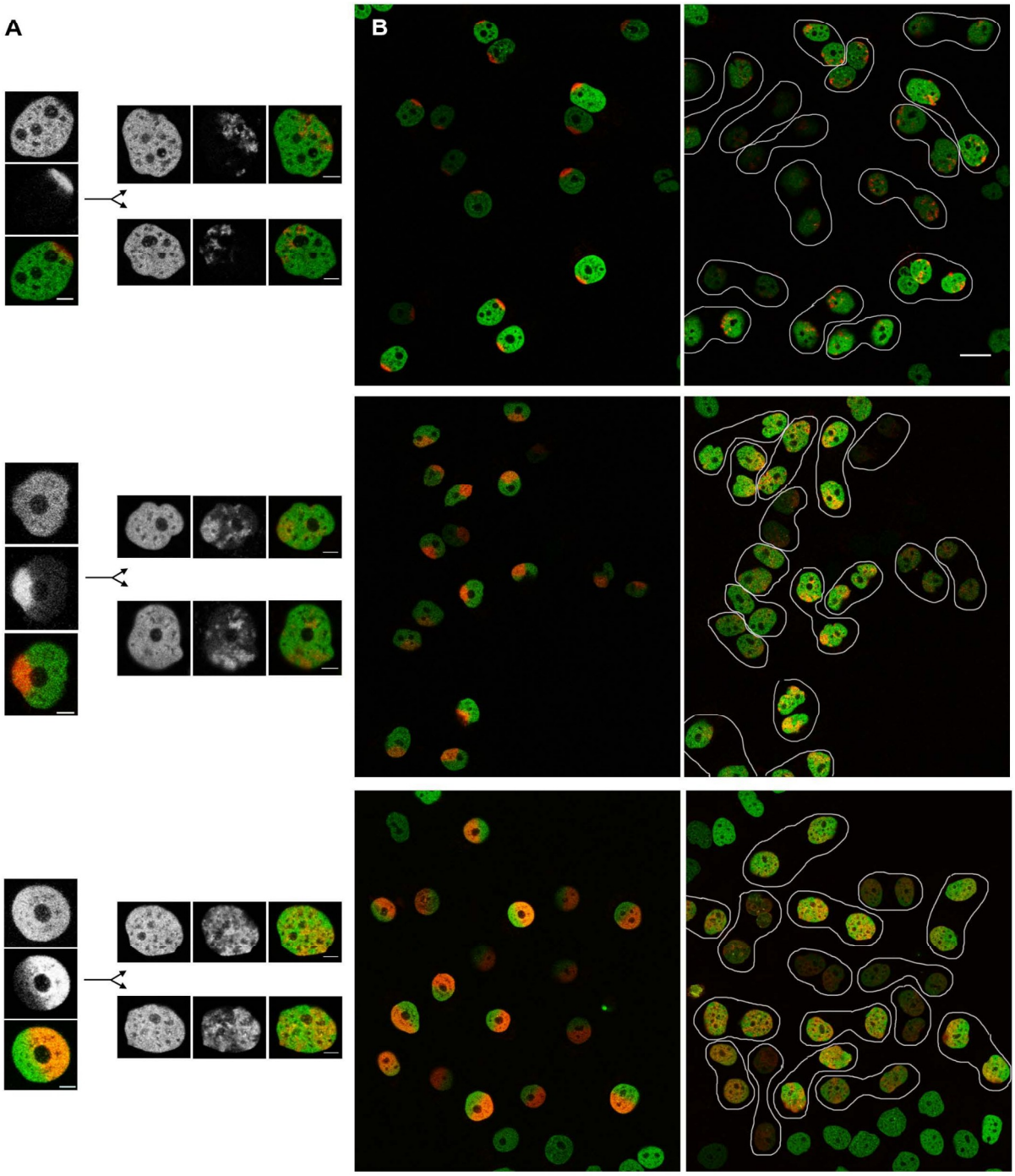

Figure 5.2 The behavior of the labeled nuclear domains of unknown composition. The behavior of the nuclear pole chromatin, the nuclear sector and the half of the nucleus is shown (consecutively) in the time-lapse experiments. Photoconversion was performed approximately 4 hours after release from the thymidine block. The time-lapses corresponded to 13, 16 and 17.5 hours, respectively. **(A)** Examples of images of the mother cell (overall chromatin, photoconverted chromatin and merged image) and the daughter cells are provided. Scale bar: 5μm.

(B) The initial and the final merged snapshots of the time-lapse are shown. The pairs of daughter cells are indicated. Note extensive changes in the distribution of label in many daughter cells. Scale bar: 20 μm.

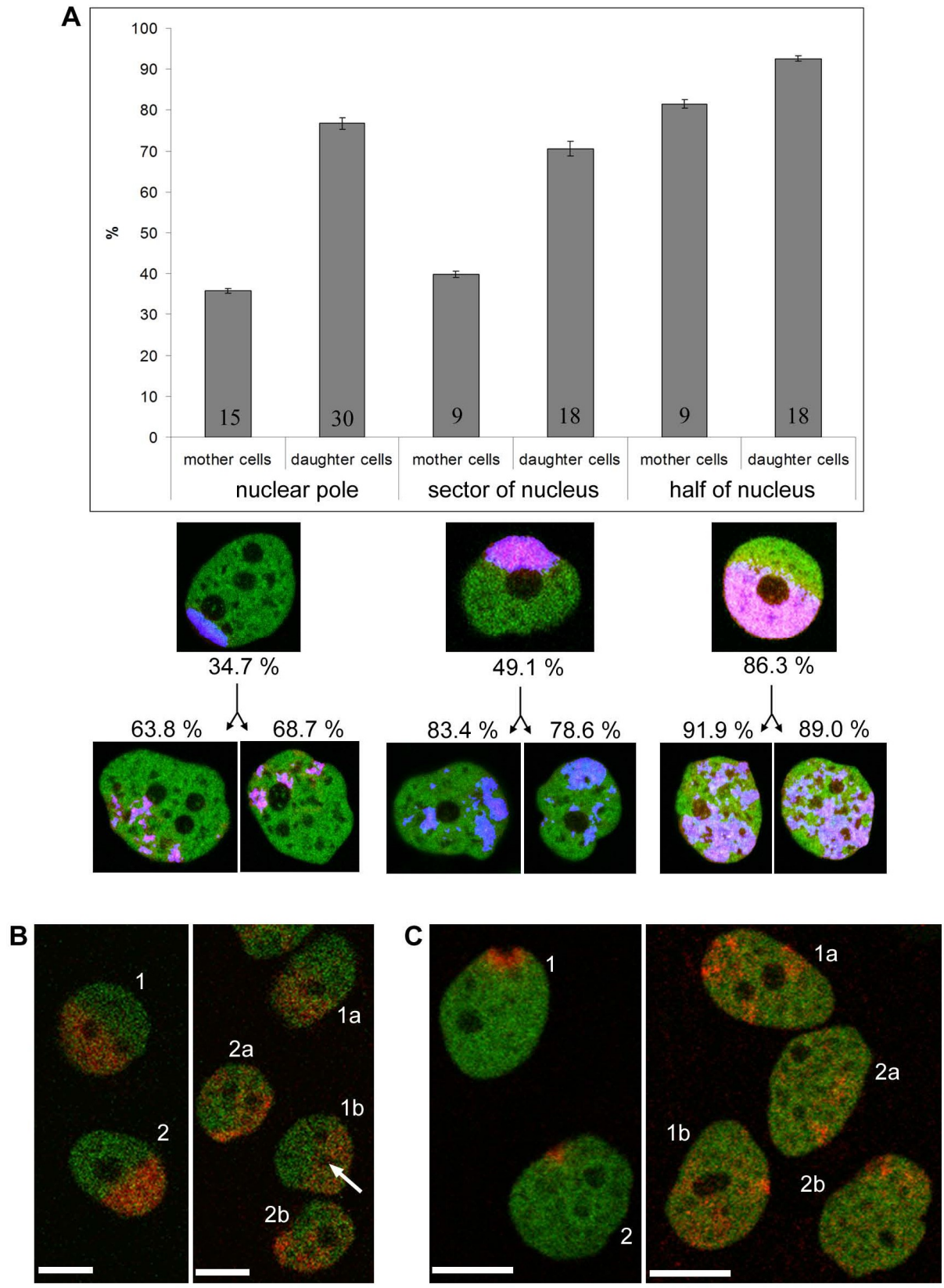

Figure 5.3 The behavior of the labeled nuclear domains of unknown composition and the quantitative evaluation of the signal distribution in mother and daughter cells.

(A) Quantitation of the threshold images (the real averaged distance is given as the percentage of the random distribution distance; the number of evaluated cells is given in individual columns) together with examples of cells shown already in Fig. 2A. The data show that the distribution of signal in daughter cells is not identical with that in mother cell but is not, at the same time, randomly scattered. **(B)** An example of the cell in which the distribution of label in the daughter cells is similar to that seen in the mother cell (relevant cells are designated as 1, 1a and 1b). Here the position of nucleoli testifies for extensive changes of the chromatin position that took place in the daughter cells. In the mother cell 1, the two nucleoli are situated at the border of the photoconverted chromatin region. However, in the daughter cell 1b, an arrow points to the nucleolus that is entirely engulfed within the labeled chromatin region. The shown images were taken 6 hours prior mitosis and 4 hours after the mitosis was completed. Scale bar: 10 μm. **(C)** Example of two mother cells in which a tiny perinuclear chromatin region was photoactivated. In the daughter cells, the label is scattered; to improve visibility of the scattered signal, the image was contrast-stretched. Live cell imaging experiment lasted 18 hours. Scale bar: 10 μm.

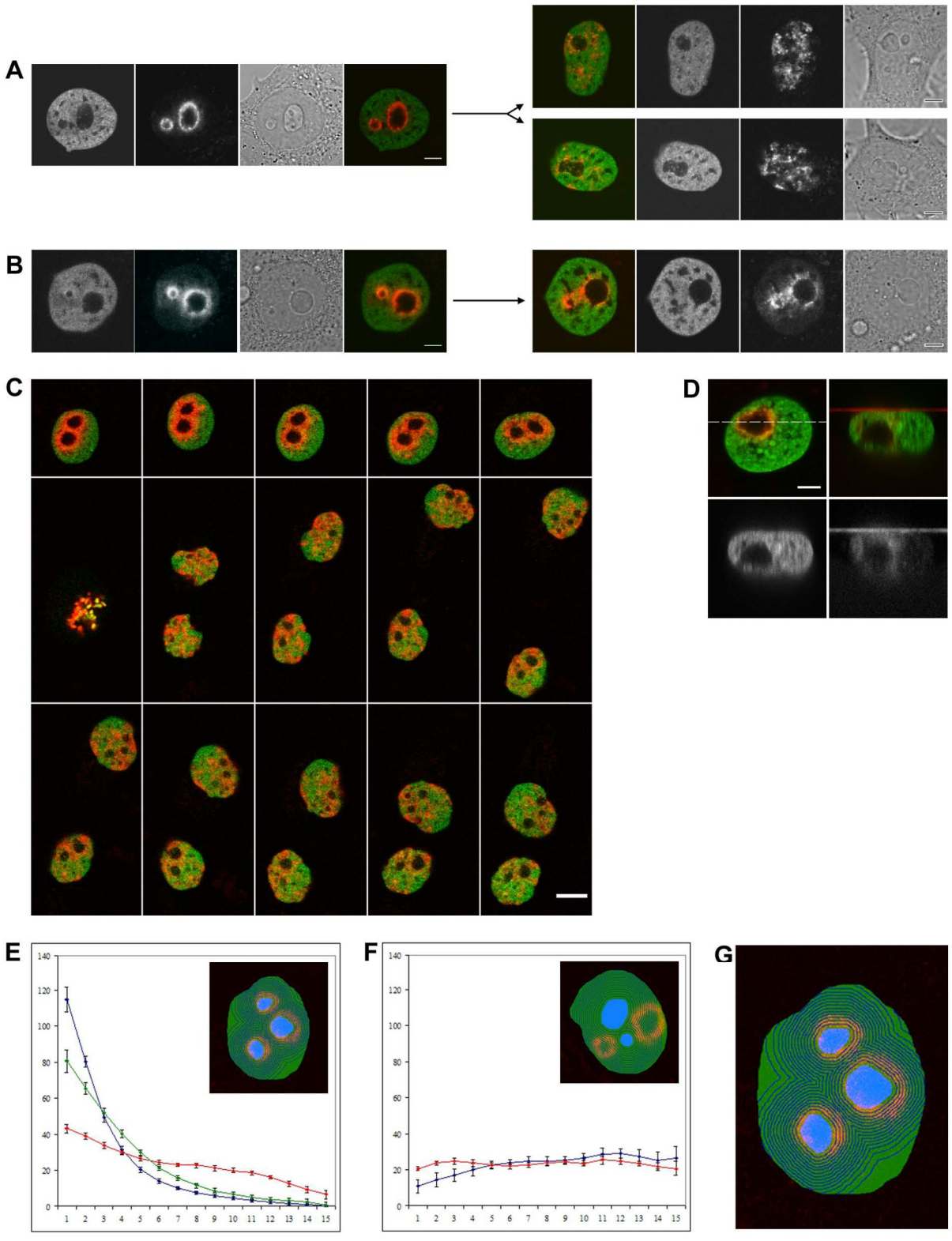

Figure 5.4 The labeling of the NAC, the behavior of the labeled NAC in live cell experiments and the quantitative evaluation of the location of the mother cell-labeled NAC with nucleoli in the daughter cells. The chromatin in the closest vicinity of nucleoli in HepG2$^{H4\text{-}Dendra2}$ cells is photoconverted in S/early G2 phase. Labeled cells

are observed by time-lapse imaging. **(A)** Initial snapshot taken just after conversion and the snapshot taken 14 hours later are documented (the two channels, the bright field and the merged image are shown). Scale bar: 5µm. **(B)** Similar as in A, but the labeled cell failed to divide during 15 hours. Scale bar: 5µm. **(C)** Time-lapse imaging of the mother cell-labeled NAC. Merged image snapshots in one hour intervals are shown. Note that during the time-lapse imaging with the focal plane fixed, the dynamic behavior of daughter cells resulted sometimes e.g. in disappearance and reappearance of nucleoli in some snapshots. Scale bar: 10µm. **(D)** Chromatin labeling at the time of photoconversion is provided. Merged image of xy section (dashed line corresponds to the plane of xz section) and xz section, as well as individual channels of converted and overall chromatin in xz sections, are shown. Scale bar: 5µm. **(E-G)** Evaluation of the distribution of the photoconverted H4-Dendra2 signal with respect to nucleoli in mother and daughter cells. Acquired images (fluorescence of non-converted and converted Dendra2; bright field pictures) are processed as described in Materials and Methods. Outcomes are dependencies of the average pixel intensity of converted Dendra2 in the given region related to the distance of the region from nucleoli borders. Blue curves represent chromatin behavior in mother cells, red curves are related to chromatin in daughter cells. Inserts in Fig. E,F illustrate segmentation of the nucleus into equivalent regions concentrically arranged around all nucleoli within the nucleus. In Fig. E, photoconverted chromatin in both mother (n=24; mean and standard deviation of the mean are given) and daughter (n=33) cells exhibits tendency to be associated with nucleoli. Green curve describes behavior of chromatin in cells which fail to divide (n=9). The area delimited below red and above green curves roughly represents a fraction (about 30 %) of photoconverted chromatin not located in the vicinity of nucleoli in daughter cells. In Fig. F, the "randomly" (i.e. not encompassing nucleoli) chosen chromatin in mother (n=8) and daughter (n=10) cells exhibits no bias for the nucleolar vicinity. In Fig. G, the detailed example of the segmentation is given.

Movie 5.1 Time-lapse imaging of the labeled NAC. The closest vicinity of nucleoli in HepG2$^{H4\text{-}Dendra2}$ cells was photoconverted in partially synchronized cells in late S/early G2 phase. Labeled cells were observed by time-lapse imaging with 30 min snapshot intervals, movie encompassed 15 hours. Merged movie of photoconverted (red) and overall chromatin (green) is shown.

The movie can be found on a CD enclosed to the printed version of the thesis.

6. PONTIN IS LOCALIZED IN NUCLEOLAR FIBRILLAR CENTERS

6.1 Introduction

The Pontin protein was described as a putative mammalian DNA-helicase containing Walker A and Walker B motifs and belonging to the family of AAA+ ATPases. Pontin was independently described by several research groups that studied diverse cellular processes in different model organisms, which resulted in many Pontin synonyms - Tip49a, Tih2p, rp50, RUVBL1, NMP 238, ECP 54, p55. As part of several protein complexes, the major role of Pontin is apparently in the regulation of chromatin structure and gene expression and in DNA repair and stability. In this context, Pontin was identified as a component of different chromatin remodeling and modifying complexes including the Tip60, Ino80 and Uri complexes (for review see Gallant, 2007). In addition, it has been shown that Pontin interacts with several transcription regulators like β-catenin, c-Myc and E2F1 and associates with the promoters targeted by these factors (Bauer et al., 1998; Bauer et al., 2000; Dugan et al., 2002; Frank et al., 2003; Taubert et al., 2004; Wood et al., 2000). Through its interaction with Hint1, Pontin modulates β-catenin mediated transcription in the canonical Wnt-signaling pathway and apoptosis (Weiske and Huber, 2005; Weiske and Huber, 2006). Besides transcriptional regulation Pontin has additional functions in maturation of small nucleolar ribonucleoprotein particles (snoRNPs) (King et al., 2001; McKeegan et al., 2007; Watkins et al., 2002; Watkins et al., 2004), in assembly of the telomerase holoenzyme complex (Venteicher et al., 2008) and through association with the mitotic spindle it appears that Pontin is involved in cell division (Gartner et al., 2003).

Several lines of evidence suggest that Pontin may act in the nucleolus: 1) Pontin interacts with c-Myc, which regulates the activity of all three RNA polymerases including RNA polymerase I (Pol I) (Arabi et al., 2005; Grandori et al., 2005), 2) Pontin is a part of the Uri complex that includes Rpb5, a protein associated with Pol I (Zaros et al., 2007) and 3) Pontin is involved in the maturation of snoRNPs that mostly reside in the nucleolus. Indeed, Pontin was detected in nucleoli by extensive proteomic analysis (Leung et al., 2006). However, direct nucleolar localization of Pontin was never observed. Here, we focused on Pontin localization in more detail using immunofluorescence and electron microscopy and showed that Pontin is localized in the nucleolus, specifically in the nucleolar fibrillar centers.

Moreover, we observed a dynamic, cell cycle-specific redistribution of Pontin within the nucleolus and found interactions between Pontin and the Pol I transcription machinery.

6.2 Materials and methods

6.2.1 Cell culture, synchronization

HeLa and HepG2 cells were cultured in Dulbecco's Modified Eagle's Medium with 10 % (v/v) fetal bovine serum and supplemented with penicillin-streptomycin. For partial cell synchronization, cells were incubated for 16 hours with 3 mM thymidine (Sigma). Thymidine was washed out to release cells into the S-phase as determined by 5-bromo-2'-deoxyuridine (BrdU) labeling one hour after thymidine removal (Koberna et al., 2005).

6.2.2 siRNA

To reduce expression levels of the Pontin protein HeLa cells were transiently transfected with two siRNA duplexes (21-mers with 3'-dTdT overhangs) as described in (Watkins et al. 2004). Following the protocol of (Elbashir et al., 2002), siRNA oligonucleotides were annealed to produce siRNA duplexes. Annealing quality of siRNA duplexes was controlled by electrophoresis on a 4 % (w/v) agarose gel. Transfection was performed with Oligofectamine (Invitrogen) according to the manufacturer's protocol. Cells were analyzed 48 and 72 hours post transfection.

6.2.3 Antibodies, immunofluorescence and light microscopy

Two monoclonal antibodies raised against Pontin were used in this study. Immunization and generation of antibodies has been reported previously (Weiske and Huber, 2005). Clones 5G3-11 and 3A4-1 were isolated by ELISA screening and specificity was tested by Western blotting of cell lysates prepared as described previously (Meyer zum Buschenfelde et al., 2006). Epitope mapping was performed with purified recombinant MBP-Pontin fusion proteins with deletions either at the N- or C-terminus (Weiske and Huber, 2005). Human autoantibodies anti-fibrillarin, anti-Upstream Binding Factor (UBF), anti-RNA polymerase I (kindly provided by Marvin Fritzler, Medical School, University of Calgary) and mouse anti-fibrillarin 17C12 (kindly provided by K.M. Pollard, The SCRIPPS Research Institute, CA; (Yang et al., 2001) were used as nucleolar markers. Rabbit anti-SART3 antibodies

(Staněk et al., 2003) were used as nucleoplasmic markers. The monoclonal anti-vimentin antibody VI-01 (Dráberová et al., 1986) was kindly provided by Pavel Dráber (Institute of Molecular Genetics, AS CR, Prague, Czech republic). The anti-c-Myc (N-262 X) was obtained from Santa Cruz Biotechnology.

For immunofluorescence detection, cells were grown on coverslips, washed with PBS, fixed in 2 % (w/v) paraformaldehyde for 10 minutes and permeabilized with 0.2 % (v/v) Triton X-100 in PBS for 5 minutes. Cells were then washed with PBS and incubated with monoclonal antibodies against Pontin diluted in 1 % (w/v) BSA in PBS for 1 hour, washed and incubated with secondary antibodies conjugated to TRITC or FITC (Jackson ImmunoResearch Laboratories) in 1 % (w/v) BSA in PBS for 1 hour. In the case of the double labeling procedure, cells were incubated for one hour with mouse anti-Pontin antibodies (5G3-11 or 3A4-1) and one of the human autoantibodies mentioned above, both diluted in 1 % (w/v) BSA in PBS, washed in PBS and incubated for another hour with a mixture of secondary anti-mouse and anti-human antibodies conjugated with TRITC and FITC, respectively. All steps were performed at room temperature.

To test the specificity of the monoclonal antibody staining, antibodies were pre-incubated in PBS containing 1 % BSA for one hour at room temperature with 5x excess of GST-Pontin fusion protein or with GST alone and subsequently used for immunofluorescence staining.

Coverslips were mounted to glycerol containing DAPI (for DNA staining) and DABCO (as an anti-fade agent). Images were taken with the Leica SP2 laser scanning confocal microscope.

6.2.4 Transcription labeling

Cell were incubated with 2 mM 5-fluorouridine (Sigma) for 10 minutes, fixed in 3.7 % (w/v) paraformaldehyde for 5 minutes and permeabilized with 1 % (v/v) Tritone X-100 in PBS for 10 minutes. Cells were then incubated with a mixture of mouse anti-Pontin (3A4-1) and rat anti-BrdU antibodies (Abcam) diluted in 1 % (w/v) BSA in PBS for one hour followed by incubation with secondary antibodies anti-mouse conjugated with TRITC and anti-rat conjugated with FITC (Jackson ImmunoResearch Laboratories).

6.2.5 Cell lysate preparation and Western blot analysis

For whole-cell lysate preparation, cells grown on Petri dishes were washed with ice-cold PBS and scraped off the dish in 2x sample buffer (2 x SB consists of 20 % (v/v) glycerol, 125 mM Tris-Cl, pH 6.8 and 4 % (w/v) SDS). Lysates were homogenized by passing through a 22G needle. Nucleoplasmic and nucleolar fractions were prepared according to a previously published protocol (Andersen et al., 2002). Protein concentration was determined using the bicinchonic acid assay. Before electrophoresis, mercaptoethanol and bromphenol blue were added to final concentrations 5 % (v/v) and 0.01 mg/ml, respectively, and samples were incubated for 5 min at 85°C. Whole-cell lysates were separated on 12 % SDS-PAGE and transferred to nitrocellulose membranes (Protran). Membranes were blocked and incubated with mouse anti-Pontin antibodies diluted in PBST containing 5 % (w/v) Blotto (Santa-Cruz Biotechnology, Inc) and then with goat anti-mouse secondary antibodies conjugated with horseradish peroxidase (Biorad) diluted in 5 % (w/v) Blotto in PBST for 1 hour at room temperature. In control experiments anti-vimentin VI-01, anti-fibrillarin 17C12 and anti-SART3 antibodies were applied, each diluted in 5 % (w/v) Blotto in PBST. Horseradish peroxidase activity was detected using an ECL chemiluminiscence system (Pierce) and captured on X-ray film (Foma). Intensity of bands was quantified by ImageJ software.

6.2.6 Electron microscopy

HeLa cells were partially synchronized to S-phase by thymidine treatment (see above) and fixed in freshly prepared 8 % (w/v) formaldehyde in 0.2 M PIPES buffer, pH 6.95 for 12 hours, washed in PBS, scraped and centrifuged at 1000 rpm for 5 minutes and mixed with 10 % (w/v) gelatin in PBS at 37°C. Cells were again centrifuged for 5 minutes at 1.000 rpm and the excess of gelatin was removed. Cells in gelatin were chilled at 4°C, fixed with 8 % (w/v) formaldehyde in 0.2 M PIPES, pH 6.95 for 20 minutes and washed in PBS. Cells embedded in gelatin were removed from centrifuge tube, and cut into small pieces (less than 1 mm^3). Cells were cryo-preserved and frozen according to protocol described previously (Raška et al., 1995). Thin cryosections were cut on the ultracut (Leica) equipped with a cryochamber. Grids with cryosections were incubated with mouse anti-Pontin (5G3-11) antibody for 30 minutes, washed in PBS, incubated with 6 nm gold anti-mouse adduct (Jackson ImmunoResearch Laboratories) for 20 minutes, washed in PBS and water,

embedded in mixture of 3 % (w/v) polyvinyl alcohol (MW. 30-70 kDa, Sigma) and 0.1 % (w/v) uranylacetate and dried. The sections were viewed using a Zeiss EM 900 electron microscope equipped with a KeenView CCD camera (Soft Imaging Systems).

6.2.7 Immunoprecipitation

$7x10^6$ cells were washed twice with ice cold PBS containing $Mg^{2+}$and incubated with 500 µl of Lysis buffer A (10 mM imidazol pH 6.8, 100 mM KCl, 300 mM sucrose, 2 mM $MgCl_2$, 10 mM EGTA, 2 % (v/v) Triton X-100, protease inhibitor cocktail (Calbiochem)) for 10 minutes on ice. Cells were removed from the plate and centrifuged at 20.800 g for 10 min. 450 µl of supernatant was immunoprecipitated with 2 µg of 3A4-1 antibody pre-bound to 30 µl of Protein-G beads under continual agitation for 4 hours at 4°C. After five washings with Lysis buffer A, the immunoprecipitated proteins were resuspended in 30 µl of 2x sample buffer and separated by 12 % SDS-PAGE.

6.2.8 Chromatin immunoprecipitation (ChIP)

HeLa cells were grown to confluency and fixed with 1 % formaldehyde for 10 min at room temperature. Subsequently, the cells were washed twice with PBS and the cross-linking reaction was stopped by incubation with glycine at a final concentration of 125 mM for 10 min, followed by washing twice with PBS. Cells were lysed by incubation in 1 ml cell-lysis buffer (5 mM Pipes pH 8, 85 mM KCl, 0.5 % (v/v) NP40, 1 mM PMSF, protease inhibitor cocktail (Roche)) for 10 min at 4°C. Subsequently, cells were scraped from the cell culture dish and nuclei were pelleted by centrifugation (2.700 x g, 5', 4°C). The pellet was resuspended in 500 µl RIPA-buffer (50 mM TrisHCl pH 8, 150 mM NaCl, 1 % (w/v) Nonidet-P40, 0.5 % (w/v) Na-Deoxicholate, 0.1 % (w/v) SDS, 1 mM PMSF and Protease inhibitor cocktail (Roche)). Nuclei were disrupted by sonication with three 20 s pulses in a UP 50H sonicator (Hielscher Ultraschall Technologie) at a setting of cycle 0.5 and 30 % amplitude, yielding genomic DNA fragments with a bulk size of 200-1000bp. For ChIP 50 µg of DNA diluted in RIPA-buffer were incubated with 2 µg anti-Pontin (5G3-11) or anti-c-Myc (N-262 X) antibodies overnight at 4°C in an orbital shaker. Immune complexes were precipitated by the addition of 35 µl Protein A-Sepharose

CL4B beads for 1h at 4°C. Precipitates were serially washed three times with RIPA-buffer, three times with high salt-buffer (100 mM Tris-HCl pH 8, 500 mM LiCl, 1 % (v/v) Nonidet-P40, 0.5 % (w/v) Na-deoxycholate, Protease inhibitor cocktail (Roche)) and twice with TE-buffer (10 mM TrisHCl pH 8, 1 mM EDTA). Precipitates were then treated with 50 ng/µl RNase A in 200 µl TE-buffer at 37°C for 1 hour. Subsequently proteins were digested by addition of 50 µl 5x Proteinase K-buffer (50 mM Tris-HCl pH 7.5, 25 mM EDTA, 1.25 % (w/v) SDS) to the RNase A-reaction and the addition of 50 ng/ml Proteinase K. Samples were incubated at 65°C overnight under constant agitation. DNA was purified by phenol/chloroform extraction and subsequent ethanol precipitation. For PCR analysis 2 µl of the extracted DNA (50 µl) was used as a template for 25-35 cycles of amplification. For the two-step ChIP assay, components were eluted from the first immunoprecipitation reaction by incubation with 10 mM dithiothreitol at 37°C for 30 min and diluted 1:40 in RIPA-buffer followed by immunoprecipitation with the second antibodies. ReChIP was essentially performed as the first ChIP. For the detection of rDNA initiator- and terminator-regions primer-sets H1 and H13 were used as described previously (Grandori et al. 2005). The following primers were used for detection of the GAPDH promoter: Forward - 5'-TACTAGCGGTTTTACGGGCG-3' and reverse - 5'-TCGAACAGGAGGAGCAGAGAGCGA-3' giving a 166bp PCR product.

6.3 Results

6.3.1 Characterization of anti-Pontin monoclonal antibodies

Monoclonal antibodies were raised against the whole Pontin protein to obtain tools for studying Pontin intracellular localization and function. Individual clones were tested for their ability to immunostain Pontin and specificity of the two selected monoclonal antibodies were further tested using whole cell lysates and immunoblotting (Fig. 6.1a). Both, the 5G3-11 and the 3A4-1 antibodies recognized a protein band with an apparent molecular weight of ~50kD that corresponds to Pontin. To further test antibody specificity, protein extracts were prepared from cells treated with siRNA against Pontin (Fig. 6.1b). A significant decrease of signal was observed in cells treated with specific siRNAs but not with negative control siRNAs. In addition, both antibodies specifically immunoprecipitated Myc-tagged Pontin from cell extracts (Fig. 6.1b). To define the regions in the Pontin protein containing the epitopes recognized by the antibodies, different Pontin deletion constructs were

bacterially expressed, purified and used for epitope mapping (Fig. 6.1d). These data demonstrate that 5G3-11 and 3A4-1 antibodies interact with different regions of the Pontin protein and specifically recognize Pontin in cellular extracts.

6.3.2 Intracellular localization of Pontin

Pontin localization has been elusive and different groups referred to diverse localization based on the antibody and/or fixation conditions used (Bauer et al., 1998; Holzmann et al., 1998; Makino et al., 1998; Salzer et al., 1999). Moreover, a GFP-tag on either end of the protein prevents Pontin localization to the nucleus (data not shown) and thus impairs studying the intranuclear distribution. Here we used two different monoclonal antibodies to analyze Pontin localization *in situ* (Fig. 6.1c). Both antibodies revealed a similar staining pattern and detected Pontin in the nucleoplasm. Surprisingly, a signal in nucleoli was also observed and a significant number of cells exhibited bright dots. Similar results were obtained with the human hepatocellular carcinoma cell line HepG2 (data not shown). Specificity of the staining was further confirmed by pre-incubation of the antibodies with GST-Pontin. Nuclear and nucleolar staining disappeared after antibody pre-incubation with GST-Pontin but not with GST alone (Fig. 6.1c).

6.3.3 Pontin dots are localized in the nucleolus

Based on DAPI staining and phase contrast, the Pontin dots appeared preferentially in nucleoli (Fig. 6.1d). To confirm this nucleolar localization, cells were double labeled with antibodies against Pontin and chosen nucleolar markers (fibrillarin, Upstream Binding Factor or RNA polymerase I; Fig. 6.2a,b). Fibrillarin associates with C/D box snoRNPs that function in site-specific 2'-*O*-methylation of pre-ribosomal RNA and is present in nucleoli and Cajal bodies. We observed partial co-localization of Pontin dots with fibrillarin inside nucleoli, but not in Cajal bodies. Fibrillarin staining often surrounded the Pontin signal. Upstream Binding Factor (UBF) and Pol I represent important factors of ribosomal DNA (rDNA) transcription machinery localized in many dots inside the nucleolus. We found that Pontin-positive nucleolar dots overlapped with the UBF/Pol I signal (Fig. 6.2a,b).

To further confirm Pontin nucleolar localization, nucleoplasmic and nucleolar fractions were prepared and Pontin was detected by immunoblotting using the 5G3-11 antibody (Fig. 6.2c). Purity of the nucleolar fraction was verified by the detection

of fibrillarin, which accumulates in the nucleolus and SART3, a nucleoplasmic protein associated with spliceosomal snRNPs that is devoid of nucleoli. Fibrillarin was not detected in the whole cell extract probably due to lower concentration of this protein in the total cell lysate. Taken together these data show that a significant fraction of Pontin is localized in nucleoli.

6.3.4 Pontin accumulates in nucleolar fibrillar centers

The nucleolus consists of three different regions: fibrillar centers, dense fibrillar components, and granular components. rDNA was mainly mapped to the fibrillar centers that also contain the rDNA transcription machinery (e.g. Pol I, UBF). In contrast, newly synthesized pre-ribosomal RNA (pre-rRNA) and factors involved in pre-rRNA processing (e.g. snoRNPs, fibrillarin) are localized in the dense fibrillar components (Raška, 2003; Raška et al., 2006a; Raška et al., 2006b). Co-localization of Pontin with Pol I and UBF indicates that Pontin is specifically localized to the fibrillar centers. However, light microscopy does not posses enough resolution to specifically address sub-nucleolar localization (Koberna et al., 2002). Therefore, we used electron microscopy to locate Pontin within the nucleolus. Thin sections from synchronized HeLa cells were incubated with anti-Pontin (5G3-11) antibody and subsequently visualized by antibodies bound to gold particles (Fig. 6.3). Labeling within the nucleolus was specifically enriched in the fibrillar centers.

6.3.5 Nucleolar localization of Pontin during S-phase

The Pontin labeling pattern differs between individual cells within an unsynchronized cell population (Fig. 6.1d). While the Pontin nucleolar signal was presented in all cells bright dots appeared only in a fraction of cells. To test whether accumulation of Pontin in the nucleolar dots is cell cycle dependent, we partially synchronized HeLa cells in S-phase by a thymidine block and stained them with monoclonal antibodies one hour after release from the thymidine block. The number of cells in S-phase was controlled in parallel experiments by labeling of newly synthesized DNA with BrdU. Almost all of the cells were in S-phase one hour after release from the thymidine block (data not shown). In S-phase, the number of cells containing Pontin nucleolar dots increased to 96 % while only 42 % of cells in the unsynchronized culture exhibited nucleolar accumulation of Pontin (Fig. 6.4a,b).

To test whether Pontin accumulation in the nucleolar dots corresponded to increased expression of the Pontin protein in S-phase, the amount of Pontin protein was analyzed in S-phase cells and in unsynchronized cell populations (Fig. 6.4c). Although the number of cells with Pontin dots significantly increased in S phase, the amount of protein did not change. These data indicate that accumulation of Pontin in big dots is rather due to its relocalization within the nucleolus than to a higher expression of the Pontin protein during S-phase.

6.3.6 Pontin interacts with the nucleolar transcription machinery

To get further inside into Pontin function in the nucleolus, immunoprecipitation with the anti-Pontin (3A4-1) antibody was performed and the association of nucleolar proteins with Pontin was analyzed (Fig. 6.5a). The anti-Pontin antibody co-precipitated Pol I but not fibrillarin or UBF. These data suggest that Pontin in the nucleolus may be involved in the regulation of rRNA synthesis. In this respect, Pontin was identified as a c-Myc co-factor that regulates activity of several genes. c-Myc was recently identified as an activator of rRNA transcription that interacts with specific regions of rDNA genes (Grandori et al. 2005). To test whether Pontin associates with c-Myc at these rDNA loci we performed chromatin immunoprecipitation (ChIP) with anti-Pontin and anti-c-Myc antibodies. Cis-elements H1 (close to the transcriptional start) and H13 (close to the termination site), which were previously identified as major c-Myc binding targets were analyzed (Fig. 6.5b). These experiments confirmed the earlier findings showing that c-Myc binds to these sites in the rDNA gene cluster (Grandori et al. 2005). In addition, our data show that Pontin is also associated with these rDNA loci. Since Pontin has been shown to interact with c-Myc and to modulate c-Myc transcriptional activity, the formation of Pontin/c-Myc complexes at these rDNA sites was analyzed by two-step ChIP. The first ChIP was performed with the anti-Pontin (5G3-11) antibody followed by a second ChIP using an anti-c-Myc antibody or vice versa (Fig. 6.5b). Both combinations gave the same result indicating that Pontin binds to rDNA cis-elements in a complex with c-Myc.

The observation that Pontin interacts with Pol I, c-Myc and rDNA indicate that Pontin is involved in the regulation of rRNA transcription. In order to analyze the relationship between nucleolar Pontin and transcription, cells were incubated for 10 min with 5-fluorouridine and newly synthesized RNA immunostained together

with Pontin and fibrillarin (Fig. 6.5c). In a few nucleoli, newly synthesized rRNA that had accumulated in the dense fibrillar components surrounded the Pontin dots, which is consistent with Pontin localization in the fibrillar centers. However, transcription was reduced in many nucleoli containing Pontin dots. Quantification of the transcription signal revealed that the accumulation of Pontin in the large nucleolar dots correlate with ~20 % reduction of nucleolar transcriptional activity.

6.4 Discussion

Pontin is a protein with many faces and its proposed functions range from chromatin remodeling and transcriptional regulation, the processing of small nucleolar RNAs, mitotic spindle function (for review see Gallant, 2007) to assembly of telomerase (Venteicher et al., 2008). Despite a large number of reports analyzing Pontin functions, a relatively few groups have analyzed Pontin cellular distribution (Bauer et al. 1998; Holzmann et al. 1998; Makino et al. 1998; Salzer et al. 1999). However, outcomes of these studies have been inconsistent. Considering the multitude of potential Pontin interactions and the number of protein complexes Pontin participates in, various localizations are likely. These discrepant results could be explained by the combination of different epitope availabilities in different complexes and antibody specificities towards these epitopes. An additional factor that may play a role in Pontin recognition is a fixation procedure that can significantly influence epitope recognition (data not shown). Depending on the combination of antibodies and fixation conditions each study might have detected different functional pools of Pontin and their results are rather complementary.

Here, we used two different monoclonal antibodies recognizing different epitopes in Pontin to determine its sub-cellular distribution. In accordance with previous studies, we detected Pontin predominantly in the cell nucleus. Surprisingly, Pontin was also found in the nucleolus. In a large number of cells, Pontin concentrated in big nucleolar dots and this localization was cell cycle dependent. Presence of Pontin in the nucleolus was further confirmed by its detection in nucleolar extracts. To determine Pontin sub-nucleolar distribution, Pontin was detected by means of electron microscopy and was found to be localized specifically to fibrillar centers. Our data are in agreement with multiple mass spectrometric analyses that found Pontin in isolated nucleoli (Leung et al., 2006) and provide the first direct visualization of Pontin in the nucleolus.

Nucleolar fibrillar centers contain proteins involved in rDNA transcription but there is overwhelming evidence that they are mostly transcriptionally inactive. It is widely believed that rDNA transcription occurs at the border of the fibrillar centers and dense fibrillar components and within the dense fibrillar components themselves (Raška et al. 2006a; Raška et al. 2006b). Pontin in the fibrillar centers may interact with the rDNA transcription machinery and regulate its activity during the cell cycle. In this respect, we found that Pontin specifically interacts with Pol I but not UBF even though both proteins are concentrated in the fibrillar centers.

It was previously shown that Pontin interacts with c-Myc and functions as a c-Myc co-activator (Bellosta et al., 2005; Etard et al., 2005; Wood et al., 2000). Recently, c-Myc was localized to nucleoli during cell serum stimulation where it stimulated the acetylation of rDNA chromatin and rRNA synthesis (Arabi et al. 2005; Grandori et al. 2005). We demonstrated that Pontin interacts with the same rDNA sequences as c-Myc and moreover, two-step ChIP experiments indicated that Pontin associated with rDNA in a complex with c-Myc (Fig. 6.5). Thus, Pontin is likely an important c-Myc co-factor regulating rDNA transcription. Based on our finding that the accumulation of Pontin in large nucleolar dots correlates with the reduction of rRNA synthesis we speculate that Pontin is a positive regulator of Pol I activity and its sequestering to transcriptionaly inactive fibrillar centers might represent a regulatory mechanism of rRNA transcription during the cell cycle.

6.5 Figures

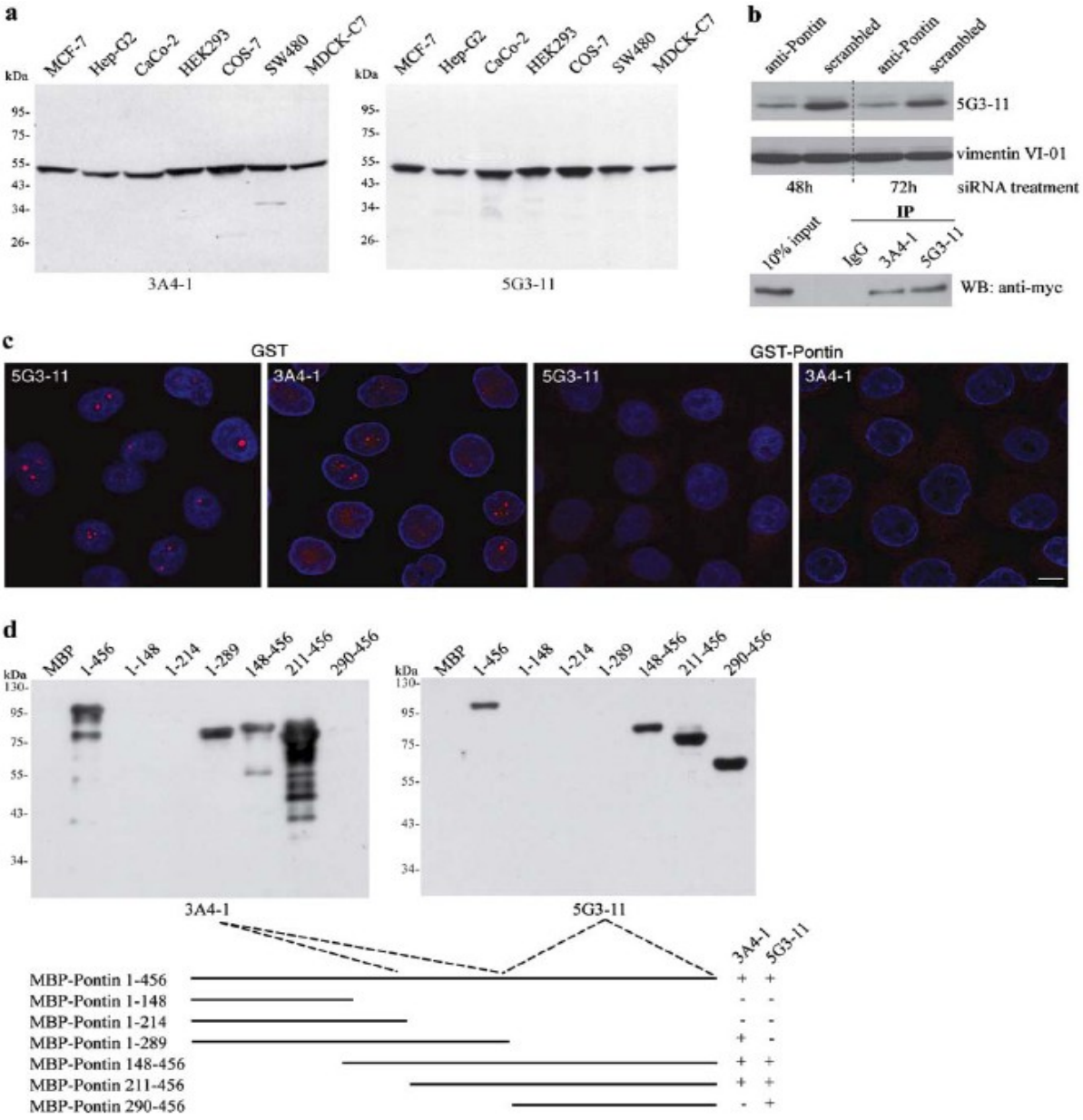

Figure 6.1 Characterization of monoclonal antibodies against Pontin. **(a)** Monoclonal antibodies were raised against the full-length recombinant protein and their specificity tested on whole cell extracts from different cell lines. Only one band of an apparent molecular weight of 50 kD is detected by either one of the antibodies. **(b)** To further confirm the antibody specificity, Pontin was detected by the anti-Pontin (5G3-11) antibody in extracts made from cells treated for 48h or 72h with anti-Pontin siRNA. A ~50 % reduction at the protein level was observed after the siRNA treatment. In addition, both anti-Pontin antibodies specifically

immunoprecipitated Myc-tagged Pontin from cell extracts. **(c)** Immunofluorescence labeling of HeLa cells with mouse anti-Pontin monoclonal antibodies (red). DNA counter-stained with DAPI (blue). Prominent dots within the nucleolus were observed in a subset of cells. Staining in the nucleus disappeared after preincubation of antibodies with GST-Pontin but not with GST alone showing the specificity of the staining. Scale bar represents 10 μm. **(d)** Different regions of Pontin were expressed in E. coli as MBP fusion proteins, purified and used for epitope mapping. The anti-Pontin (3A4-1) antibody interacts with an epitope between the Walker A and B motifs of the protein (amino acids 214-289) while anti-Pontin (5G3-11) antibody binds to an epitope within the C-terminal amino acids 290-456.

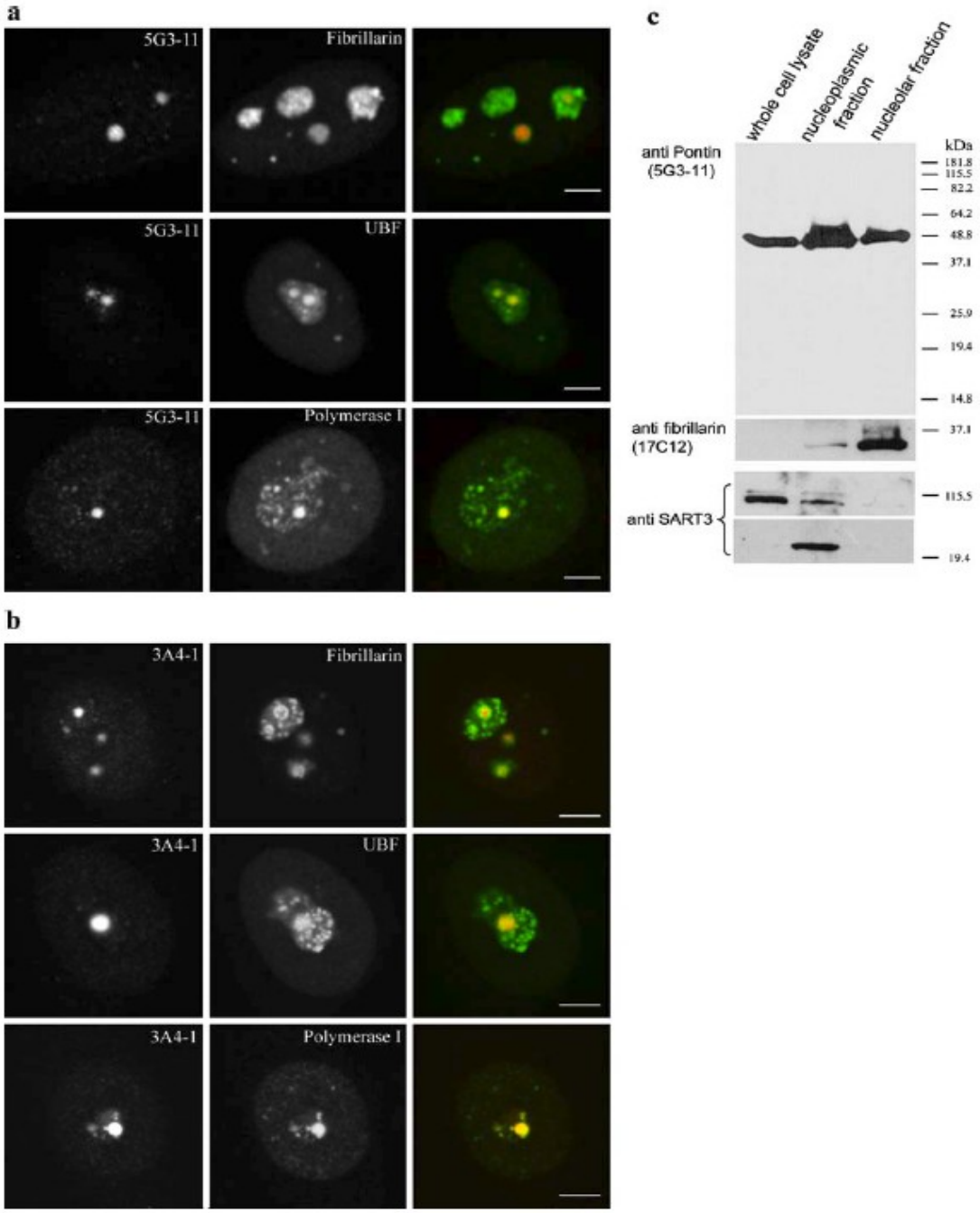

Figure 6.2 Pontin is localized in nucleoli. Double-labeling of HeLa cells with anti-Pontin antibodies 5G3-11 **(a)** or 3A4-1 **(b)** and anti-fibrillarin, anti-UBF or anti-RNA polymerase I antibodies. The large Pontin dots co-localize with UBF and RNA polymerase I containing dots. In contrast, Pontin revealed only partial co-localization with fibrillarin, which often formed a rim around Pontin dots. Note that in contrast to the three standard nucleolar proteins Pontin dots appear only in a subset of nucleoli. Scale bar represents 5 μm. **(c)** Whole cell lysate, nucleoplasmic and nucleolar

fractions were prepared and used for immunoblotting with the anti-Pontin (5G3-11) antibody. Purity of the nucleolar fraction was verified by detection of a nucleolar marker fibrillarin and absence of the SART3 protein, which is present only in the nucleoplasm and devoid of the nucleolus. SART3 was partially cleaved during the nuclear preparation and a lower molecular weight band appeared in the nucleoplasmic fraction.

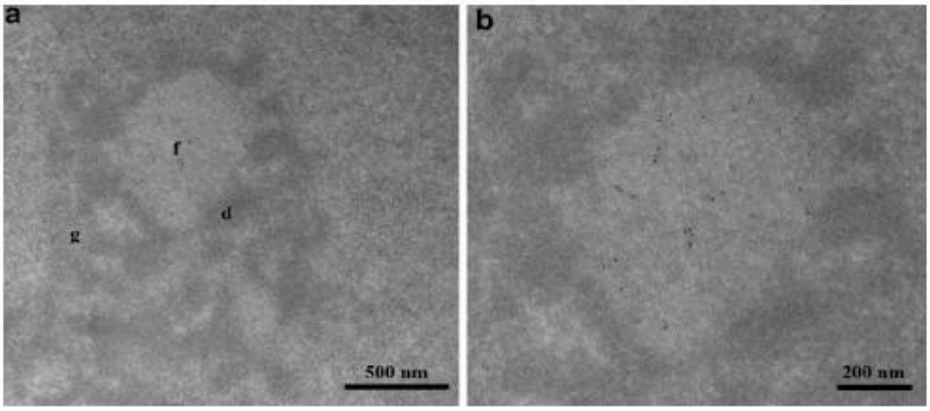

Figure 6.3 Ultrastructural localization of Pontin. **(a)** HeLa cells were synchronized in S-phase and Pontin was detected by the anti-Pontin (5G3-11) monoclonal antibody by means of electron microscopy. In this nucleolar section, Pontin is specifically enriched in a fibrillar center. **(b)** Detail of picture (a). f - fibrillar centers, d - dense fibrillar components, g - granular components.

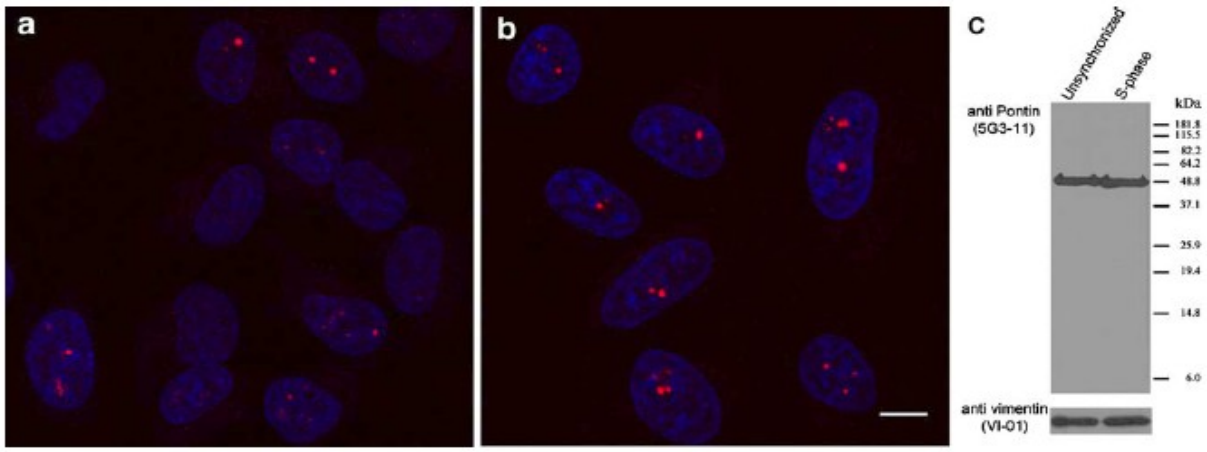

Figure 6.4 Pontin accumulates in the nucleolar dots during S-phase. Pontin was immunodetected by the anti-Pontin (5G3-11) antibody in **(a)** unsynchronized cell population or **(b)** cells synchronized to S-phase of the cell cycle. 96 % of cells in S-phase accumulated Pontin in the nucleolus. Scale bar represents 10 μm. **(c)** Equivalent amounts of proteins from S-phase cells and from unsynchronized cells were loaded in each line (vimentin antibody used as a loading control). No significant differences in protein levels of Pontin were observed between the unsynchronized and synchronized cell populations.

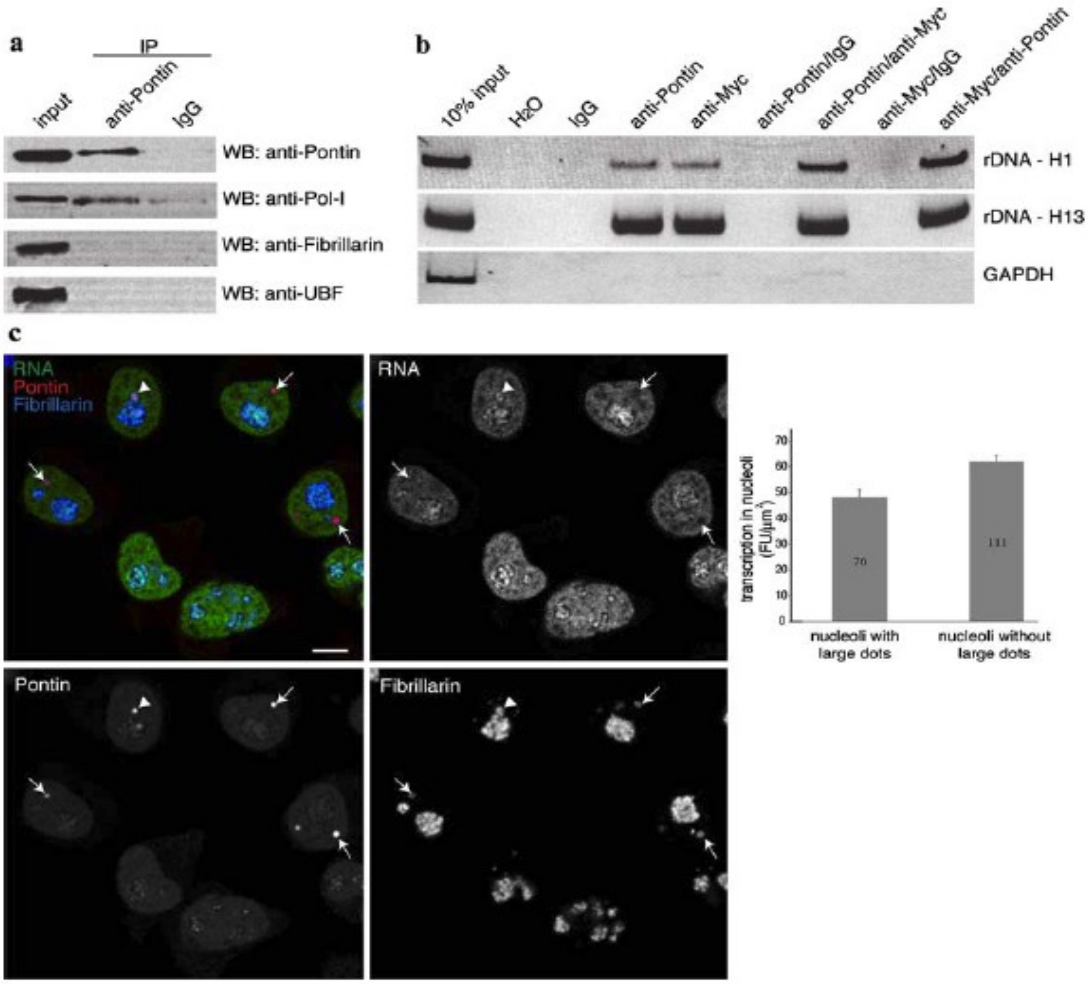

Figure 6.5 Pontin is involved in the regulation of rRNA transcription. **(a)** Pontin was immunoprecipitated using the anti-Pontin (3A4-1) antibody and nuclear proteins detected by immunoblotting. Pol I was specifically precipitated with anti-Pontin antibody but not with a control antibody. **(b)** rDNA loci H1 close to the transcription initiation site (952-1030bp) and H13 close to the termination site (12855-12970bp) were enriched after chromatin immunoprecipitation with anti-Pontin (5G3-11) or anti-Myc antibodies. Moreover, both regions were specifically amplified after two-step immunoprecipitation with anti-Pontin/anti-Myc or anti-Myc/anti-Pontin antibodies but not with control IgG antibodies showing that Pontin and c-Myc binds to the same regions of rDNA in a complex. Constitutively active GAPDH promoter served as a negative control. **(c)** Transcriptional activity of nucleoli containing large Pontin dots is reduced. Newly synthesized RNA (green) was labeled by 10 min incubation with 5-fluorouridine and visualized together with Pontin (red) and

fibrillarin (blue) as a marker of nucleoli. In transcriptionally active nucleoli, rRNA signal surrounded Pontin labelling (arrowhead). However, most nucleoli that contained Pontin dots exhibited reduce transcription activity (arrows). Quantification of nucleolar transcription (fibrillarin signal was used as a mask) revealed that transcription activity was reduced by ~20 % in nucleoli where Pontin is sequestered in large dots (average nucleolar fluorescence of transcription signal with standard error of the mean is shown together with number of nucleoli analyzed).

7. GENERAL DISCUSSION

The results presented in this thesis have settled, at least in HepG2 cells, the problem of the maintenance/non-maintenance of the chromosome organization during the cell cycle and provided new clues concerning the role of the protein Pontin in the nucleolus. The results were separately discussed in the chapters 5 and 6.

The research presented in the chapter 5 shed a new, entirely consistent light on a very important and at the same time controversial question of whether the chromatin (chromosome) position, together with its neighborhood, seen in the mother cell is maintained in the daughter cells. We used a novel labeling technique, which represents one of the first uses of the photoconvertible Dendra2 protein. Even though just HepG2 cells were investigated, we are confident that similar results are to be obtained with other human transformed cells. Still it would be worthwhile that analogous experiments with cultured human primary cells are performed. However it may be a hardly solvable problem as it is difficult to generate stably transfected cell lines with such cells because of their short live-span.

Recently, numerous claims appeared stating that genes located remote from each other on the same chromosome or even on different chromosomes show congression in the nuclear space and transient interactions as a new type of gene regulation ("gene kissing"). To better understand the implications of claims of transient or permanent "gene kisses" it is important to know to which extent certain CT neighborhoods may be probabilistic or deterministic in different cell types.

The approach of *in vivo* chromatin labeling via photoconvertible fluorescent proteins fused to core histones and time-lapse using the optimal conditions for cultured living cells is nowadays the top one. In my opinion, this technique is still too rough to distinguish finesses between labeled and unlabeled signal. It is extremely difficult to label very small regions of chromatin (few kilobases of DNA) that do not enable to detect positive signal in daughter cells. This limits our approach to study larger chromatin areas. Nevertheless, the results of our study (chapter 5) are important as several most influential cell biology groups claimed the "inheritance" of chromosome position in daughter cells (Essers et al., 2005; Gerlich et al., 2003). We have univocally established that such a strong claim of "inheritance" does not apply. Interestingly in this respect, the graph within the Fig. 5.3 is possibly the most

illustrative to shed light on this problem. It may be that these cell biology groups, using large labeled chromatin domains (particularly the half of the nucleus) just overlooked the non-maintenance of chromatin position due to "small" changes in the distribution of chromatin in daughter cells as compared to the mother cells.

It would be interesting to have a look at other regions of “specialized” chromatin, e.g., chromatin from the vicinity of nuclear bodies (visualized by their marker proteins fused to fluorescent proteins) or to label replication foci or “transcriptional factories”. The trend in microscopy techniques is favorable as the diffraction limit was broken and the resolution improved. Moreover, the usage of STED nanoscopy of fluorescent protein-labeled organelle inside a living cell was recently reported (Hein et al., 2008), indicating that newest techniques are no more restricted for fixed samples.

In chapter 6 we described in detail the intranuclear localization of Pontin, which has been so far an enigmatic multifunctional protein playing important roles in many basic nuclear processes. Functional subcompartments of the nucleoli are not yet entirely characterized and much controversy remains with assigning nucleolar subcompartments to multiple specific functions. It is important to elucidate the molecular composition of nucleolar subcompartments and to learn the role of individual proteins and complexes in nucleolar functions. This study provides the initial characterization of Pontin subnucleolar localization, which is an important step to achieve this goal. Generation of new specific antibodies greatly assisted efforts towards understanding the function of Pontin. Importantly in this respect, the two new anti-Pontin antibodies worked well by immunofluorescence as well as Western blot and that they could be also used for immunoprecipitation.

Recently, it was shown that nucleolus has many functions beyond the ribosomes generation. The identification of over 3000 proteins that are stably co-purified with isolated nucleoli might be the clue for unraveling the important processes that take place in this nucleolar organelle. The bioinformatics analysis of putative functions of these proteins complemented by localization and functional studies will help in a more detailed structure-function understanding of this important nuclear organelle.

8. CONCLUSIONS

Following conclusions were reached in the chapter 5:

- DNA construct coding the fusion protein histone H4 and photoconvertible protein Dendra2 (H4-Dendra2) was prepared.

- The stable cell line expressing H4-Dendra2 fusion protein was established from human hepatocellular carcinoma HepG2 cells.

- Functionality of H4-Dendra2 construct was confirmed in transfected HepG2 cells through a series of biological experiments and protein band corresponding to H4-Dendra2 was detected with anti-H4 and anti-Dendra2 antibodies in immunoblots.

- The live cell imaging experiments were standardized to enable $HepG2^{H4\text{-}Dendra2}$ cells observation including their passage through mitosis.

- Protein Dendra2 in H4-Dendra2 fusion was photoconverted with 405 nm laser line within the nuclear region of interest. Subsequent time-lapse experiment revealed that chromatin labeled pattern remained largely unchanged during interphase.

- Different regions of chromatin as in previously published studies were labeled by Dendra2 photoconversion: the nuclear pole, the sector and the half of the nucleus. Position of such labeled general regions of chromatin was compared in mother and daughter cells. Acquired images were thresholded and the distribution of photoconverted signal of Dendra2 evaluated. Quantification of distribution of labeled chromatin in daughter cells was shown to be significantly different with respect to mother cells, even though it was still non-random. The positioning of chromatin is thus not "inherited" in daughter cells.

- Looking at nucleoli we found that most pairs of daughter cells exhibit different numbers of nucleoli. This important common sense finding is not in harmony with the concept of "inheritance" of the chromatin positioning.

- The focus was put on the behavior of the nucleolus-associated chromatin (NAC) and its preservation through mitosis. NAC was labeled by Dendra2 photoconversion in the closest vicinity of nucleoli and time-lapse experiment followed. In agreement with known behavior of NOR-bearing chromosomes, quantification of acquired images of mother and daughter cells revealed that approximately 70 % of labeled chromatin in mother cells appeared in the vicinity of nuclei in daughter cells. Importantly, 30 % of signal was lost from the vicinity of nucleoli and the pattern of the labeled chromatin largely differed from that seen in the mother cells. Thus, these findings are not in agreement with the "inheritance" of chromatin positioning.

Following conclusions were reached in the chapter 6:

- Monoclonal antibodies (5G3-11 and 3A4-1) were raised against the whole Pontin protein to obtain tools for studying Pontin intracellular localization and function.

- Using whole-cell lysates and immunoblotting, both antibodies recognized a protein band with an apparent molecular weight of ~ 50 kDa that corresponds to Pontin.

- The specificity of these two monoclonal antibodies was verified by siRNA against Pontin as a significant decrease of signal on immunoblot was observed in cells treated with specific siRNA but not with negative control siRNA. In addition, GST-Pontin fusion protein preincubation prior to immunofluorescence labeling led to the disaperance of the label (labeling disappeared after antibody pre-incubation with GST-Pontin but not with GST alone).

- Immunofluorescence labeling of HeLa cells with the two kinds of the mouse anti-Pontin antibodies revealed the compatible labeling pattern and detected Pontin in the nucleoplasm. At the same time, cells exhibited also signal in nucleoli in the form of numerous bright dots.

- Double-labeling with anti-Pontin antibodies (either 5G3-11 or 3A4-1) and antibodies against nucleolar proteins showed a colocalization of Pontin dots with UBF and Polymerase I. In contrast, Pontin revealed only partial colocalization with fibrillarin that often formed rim around Pontin dots. These experiments (as well as experiments mentioned above) also showed that Pontin dots appear only in the subset of nucleoli.

- Pontin nucleolar localization was further confirmed by nucleoplasmic and nucleolar fractions preparation followed by immunoblotting with anti-Pontin antibodies.

- By means of electron microscopy, Pontin was shown to be specifically enriched in nucleolar fibrillar centers.

- Using immunofluorescence performed on synchronized cells, it was shown that the number of cells with Pontin dots significantly increased during S-phase. At the same time, the amount of Pontin protein, as shown by Western blotting, did not change. These data indicated that accumulation of Pontin in big dots is rather due to its relocalization within the nucleus than to its higher expression during S-phase.

- Immunoprecipitation of Pontin with anti-Pontin 3A4-1 antibody followed by detection of nuclear protein by immunoblotting revealed that Polymerase I was specifically immunoprecipitated with anti-Pontin antibody but not with a control antibody.

- Chromatin immunoprecipitation with anti-Pontin and anti-c-Myc antibodies at rDNA loci confirmed earlier findings that c-Myc binds to rDNA gene cluster and in addition showed that Pontin also associate with these rDNA loci.

- The relationship between nucleolar Pontin and transcription activity (detected by 5-fluorouridine labeling) was investigated. Quantification of the transcriptional signal revealed that the accumulation of Pontin in large nucleolar dots correlates with ~20 % reduction of transcriptional activity.

9. SUMMARY

The major aim of submitted thesis was to expand the knowledge about chromatin and the most prominent suborganelle in the cell nucleus, the nucleolus. In the first part of the thesis, we addressed a question whether the position of chromatin is conserved across mitosis in daughter cells and we focused on the behavior of the nucleolus-associated chromatin. In the second part of the thesis, we studied nucleolar localization and provided clues concerning the function of the Pontin protein.

Mammalian chromosomes occupy chromosome territories within nuclear space the positions of which are generally accepted as non-random. However, it is still controversial whether position of chromosome territories/chromatin is maintained in daughter cells. We addressed this issue and investigated maintenance of various chromatin regions of unknown composition as well as nucleolus-associated chromatin, a significant part of which is composed of nucleolus organizer region-bearing chromosomes. The photoconvertible histone H4-Dendra2 was used to label such regions in transfected HepG2 cells, and its position was followed up to next interphase. The distribution of labeled chromatin in daughter cells exhibited a non-random character. However, its distribution in a vast majority of daughter cells extensively differed from the original ones and the labeled nucleolus-associated chromatin differently located into the vicinity of different nucleoli. Therefore, our results were not consistent with a concept of preservation chromatin position. This conclusion was supported by the finding that the numbers of nucleoli significantly differed between the two daughter cells. Our results support a view that while the transfected daughter HepG2 cells maintain some features of the parental cell chromosome organization, there is also a significant stochastic component associated with reassortment of chromosome territories/chromatin that results in their positional rearrangements.

Pontin is a multifunctional protein having roles in various cellular processes including regulation of gene expression. Here we addressed Pontin intracellular localization using two different monoclonal antibodies directed against different Pontin epitopes. For the first time, Pontin was directly visualized in nucleoli where it co-localizes with Upstream Binding Factor and RNA polymerase I. Nucleolar localization of Pontin was confirmed by its detection in nucleolar extracts and by

electron microscopy, which revealed Pontin accumulation specifically in the nucleolar fibrillar centers. Pontin localization in the nucleolus was dynamic and Pontin accumulated in large nucleolar dots mainly during S-phase. Pontin concentration in the large nucleolar dots correlated with reduced transcriptional activity of nucleoli. In addition, Pontin was found to associate with RNA polymerase I and to interact in a complex with c-Myc with rDNA sequences indicating that Pontin is involved in the c-Myc-dependent regulation of rRNA synthesis.

10. REFERENCES

Ahmad, K., and S. Henikoff. 2002. The histone variant H3.3 marks active chromatin by replication-independent nucleosome assembly. *Mol Cell*. 9:1191-200.

Andersen, J.S., C.E. Lyon, A.H. Fox, A.K. Leung, Y.W. Lam, H. Steen, M. Mann, and A.I. Lamond. 2002. Directed proteomic analysis of the human nucleolus. *Curr Biol*. 12:1-11.

Ando, R., H. Hama, M. Yamamoto-Hino, H. Mizuno, and A. Miyawaki. 2002. An optical marker based on the UV-induced green-to-red photoconversion of a fluorescent protein. *Proc Natl Acad Sci U S A*. 99:12651-6.

Ando, R., H. Mizuno, and A. Miyawaki. 2004. Regulated fast nucleocytoplasmic shuttling observed by reversible protein highlighting. *Science*. 306:1370-3.

Andrews, P.D., I.S. Harper, and J.R. Swedlow. 2002. To 5D and beyond: quantitative fluorescence microscopy in the postgenomic era. *Traffic*. 3:29-36.

Arabi, A., S. Wu, K. Ridderstrale, H. Bierhoff, C. Shiue, K. Fatyol, S. Fahlen, P. Hydbring, O. Soderberg, I. Grummt, L.G. Larsson, and A.P. Wright. 2005. c-Myc associates with ribosomal DNA and activates RNA polymerase I transcription. *Nat Cell Biol*. 7:303-10.

Axelrod, D., N.L. Thompson, and T.P. Burghardt. 1983. Total internal inflection fluorescent microscopy. *J Microsc*. 129:19-28.

Bao, Y., and X. Shen. 2007. INO80 subfamily of chromatin remodeling complexes. *Mutat Res*. 618:18-29.

Bauer, A., O. Huber, and R. Kemler. 1998. Pontin52, an interaction partner of beta-catenin, binds to the TATA box binding protein. *Proc Natl Acad Sci U S A*. 95:14787-92.

Bauer, A., S. Chauvet, O. Huber, F. Usseglio, U. Rothbacher, D. Aragnol, R. Kemler, and J. Pradel. 2000. Pontin52 and reptin52 function as antagonistic regulators of beta-catenin signalling activity. *Embo J*. 19:6121-30.

Bellosta, P., T. Hulf, S. Balla Diop, F. Usseglio, J. Pradel, D. Aragnol, and P. Gallant. 2005. Myc interacts genetically with Tip48/Reptin and Tip49/Pontin to control growth and proliferation during Drosophila development. *Proc Natl Acad Sci U S A*. 102:11799-804.

Belmont, A.S., S. Dietzel, A.C. Nye, Y.G. Strukov, and T. Tumbar. 1999. Large-scale chromatin structure and function. *Curr Opin Cell Biol*. 11:307-11.

Berr, A., and I. Schubert. 2007. Interphase chromosome arrangement in Arabidopsis thaliana is similar in differentiated and meristematic tissues and shows a transient mirror symmetry after nuclear division. *Genetics*. 176:853-63.

Betzig, E., G.H. Patterson, R. Sougrat, O.W. Lindwasser, S. Olenych, J.S. Bonifacino, M.W. Davidson, J. Lippincott-Schwartz, and H.F. Hess. 2006. Imaging intracellular fluorescent proteins at nanometer resolution. *Science*. 313:1642-5.

Bickmore, W.A., and J.R. Chubb. 2003. Dispatch. Chromosome position: now, where was I? *Curr Biol*. 13:R357-9.

Boisvert, F.M., S. van Koningsbruggen, J. Navascues, and A.I. Lamond. 2007. The multifunctional nucleolus. *Nat Rev Mol Cell Biol*. 8:574-85.

Bolzer, A., G. Kreth, I. Solovei, D. Koehler, K. Saracoglu, C. Fauth, S. Muller, R. Eils, C. Cremer, M.R. Speicher, and T. Cremer. 2005. Three-dimensional maps of all chromosomes in human male fibroblast nuclei and prometaphase rosettes. *PLoS Biol*. 3:e157.

Boveri, T. 1909. Die blastomerenkerne von ascaris megalocephala und die theorie der chromosomenindividualität. *Archiv fűr Zellforschung* 3:181-268.

Boyle, S., S. Gilchrist, J.M. Bridger, N.L. Mahy, J.A. Ellis, and W.A. Bickmore. 2001. The spatial organization of human chromosomes within the nuclei of normal and emerin-mutant cells. *Hum Mol Genet*. 10:211-9.

Branco, M.R., and A. Pombo. 2006. Intermingling of chromosome territories in interphase suggests role in translocations and transcription-dependent associations. *PLoS Biol*. 4:e138.

Bridger, J.M., S. Boyle, I.R. Kill, and W.A. Bickmore. 2000. Re-modelling of nuclear architecture in quiescent and senescent human fibroblasts. *Curr Biol*. 10:149-52.

Busch, H., and K. Smetana. 1970. The nucleolus. *Academic Press, New York*.

Cavalli, G. 2007. Chromosome kissing. *Curr Opin Genet Dev*. 17:443-50.

Clemson, C.M., L.L. Hall, M. Byron, J. McNeil, and J.B. Lawrence. 2006. The X chromosome is organized into a gene-rich outer rim and an internal core containing silenced nongenic sequences. *Proc Natl Acad Sci U S A*. 103:7688-93.

Cremer, M., K. Kupper, B. Wagler, L. Wizelman, J. von Hase, Y. Weiland, L. Kreja, J. Diebold, M.R. Speicher, and T. Cremer. 2003. Inheritance of gene density-related higher order chromatin arrangements in normal and tumor cell nuclei. *J Cell Biol*. 162:809-20.

Cremer, M., J. von Hase, T. Volm, A. Brero, G. Kreth, J. Walter, C. Fischer, I. Solovei, C. Cremer, and T. Cremer. 2001. Non-random radial higher-order chromatin arrangements in nuclei of diploid human cells. *Chromosome Res*. 9:541-67.

Cremer, T., and C. Cremer. 2001. Chromosome territories, nuclear architecture and gene regulation in mammalian cells. *Nat Rev Genet*. 2:292-301.

Cremer, T., G. Kreth, H. Koester, R.H. Fink, R. Heintzmann, M. Cremer, I. Solovei, D. Zink, and C. Cremer. 2000. Chromosome territories, interchromatin domain compartment, and nuclear matrix: an integrated view of the functional nuclear architecture. *Crit Rev Eukaryot Gene Expr*. 10:179-212.

Croft, J.A., J.M. Bridger, S. Boyle, P. Perry, P. Teague, and W.A. Bickmore. 1999. Differences in the localization and morphology of chromosomes in the human nucleus. *J Cell Biol*. 145:1119-31.

Cvačková, Z., K.F. Albring, K. Koberna, A. Ligasová, O. Huber, I. Raška, and D. Staněk. 2008. Pontin is localized in nucleolar fibrillar centers. *Chromosoma*. 117:487-97.

Denegri, M., D. Moralli, M. Rocchi, M. Biggiogera, E. Raimondi, F. Cobianchi, L. De Carli, S. Riva, and G. Biamonti. 2002. Human chromosomes 9, 12, and 15 contain the nucleation sites of stress-induced nuclear bodies. *Mol Biol Cell*. 13:2069-79.

Diaspro, A., P. Bianchini, G. Vicidomini, M. Faretta, P. Ramoino, and C. Usai. 2006. Multi-photon excitation microscopy. *Biomed Eng Online*. 5:36.

Dráberová, E., P. Dráber, F. Havlíček, and V. Viklický. 1986. A common antigenic determinant of vimentin and desmin defined by monoclonal antibody. *Folia Biol (Praha)*. 32:295-303.

Dugan, K.A., M.A. Wood, and M.D. Cole. 2002. TIP49, but not TRRAP, modulates c-Myc and E2F1 dependent apoptosis. *Oncogene*. 21:5835-43.

Dundr, M., and T. Misteli. 2001. Functional architecture in the cell nucleus. *Biochem J*. 356:297-310.

Elbashir, S.M., J. Harborth, K. Weber, and T. Tuschl. 2002. Analysis of gene function in somatic mammalian cells using small interfering RNAs. *Methods*. 26:199-213.

Essers, J., W.A. van Cappellen, A.F. Theil, E. van Drunen, N.G. Jaspers, J.H. Hoeijmakers, C. Wyman, W. Vermeulen, and R. Kanaar. 2005. Dynamics of relative chromosome position during the cell cycle. *Mol Biol Cell*. 16:769-75.

Etard, C., D. Gradl, M. Kunz, M. Eilers, and D. Wedlich. 2005. Pontin and Reptin regulate cell proliferation in early Xenopus embryos in collaboration with c-Myc and Miz-1. *Mech Dev*. 122:545-56.

Federico, C., C.D. Cantarella, P. Di Mare, S. Tosi, and S. Saccone. 2008. The radial arrangement of the human chromosome 7 in the lymphocyte cell nucleus is associated with chromosomal band gene density. *Chromosoma*. 117:399-410.

Frank, S.R., T. Parisi, S. Taubert, P. Fernandez, M. Fuchs, H.M. Chan, D.M. Livingston, and B. Amati. 2003. MYC recruits the TIP60 histone acetyltransferase complex to chromatin. *EMBO Rep*. 4:575-80.

Fraser, P., and W. Bickmore. 2007. Nuclear organization of the genome and the potential for gene regulation. *Nature*. 447:413-7.

Frey, M.R., A.D. Bailey, A.M. Weiner, and A.G. Matera. 1999. Association of snRNA genes with coiled bodies is mediated by nascent snRNA transcripts. *Curr Biol*. 9:126-35.

Gallant, P. 2007. Control of transcription by Pontin and Reptin. *Trends Cell Biol*. 17:187-92.

Gartner, W., J. Rossbacher, B. Zierhut, T. Daneva, W. Base, M. Weissel, W. Waldhausl, M.S. Pasternack, and L. Wagner. 2003. The ATP-dependent helicase RUVBL1/TIP49a associates with tubulin during mitosis. *Cell Motil Cytoskeleton*. 56:79-93.

Gerlich, D., J. Beaudouin, B. Kalbfuss, N. Daigle, R. Eils, and J. Ellenberg. 2003. Global chromosome positions are transmitted through mitosis in mammalian cells. *Cell*. 112:751-64.

Gerlich, D., and J. Ellenberg. 2003. Dynamics of chromosome positioning during the cell cycle. *Curr Opin Cell Biol*. 15:664-71.

Gonda, K., J. Fowler, N. Katoku-Kikyo, J. Haroldson, J. Wudel, and N. Kikyo. 2003. Reversible disassembly of somatic nucleoli by the germ cell proteins FRGY2a and FRGY2b. *Nat Cell Biol*. 5:205-10.

Grandori, C., N. Gomez-Roman, Z.A. Felton-Edkins, C. Ngouenet, D.A. Galloway, R.N. Eisenman, and R.J. White. 2005. c-Myc binds to human ribosomal DNA and stimulates transcription of rRNA genes by RNA polymerase I. *Nat Cell Biol*. 7:311-8.

Gurskaya, N.G., V.V. Verkhusha, A.S. Shcheglov, D.B. Staroverov, T.V. Chepurnykh, A.F. Fradkov, S. Lukyanov, and K.A. Lukyanov. 2006. Engineering of a monomeric green-to-red photoactivatable fluorescent protein induced by blue light. *Nat Biotechnol*. 24:461-5.

Gustafsson, M.G. 2000. Surpassing the lateral resolution limit by a factor of two using structured illumination microscopy. *J Microsc*. 198:82-7.

Heim, R., D.C. Prasher, and R.Y. Tsien. 1994. Wavelength mutations and posttranslational autoxidation of green fluorescent protein. *Proc Natl Acad Sci U S A*. 91:12501-4.

Hein, B., K.I. Willig, and S.W. Hell. 2008. Stimulated emission depletion (STED) nanoscopy of a fluorescent protein-labeled organelle inside a living cell. *Proc Natl Acad Sci U S A*. 105:14271-6.

Hell, S.W. 2003. Toward fluorescence nanoscopy. *Nat Biotechnol*. 21:1347-55.
Hernandez-Verdun, D., P. Roussel, and J. Gebrane-Younes. 2002. Emerging concepts of nucleolar assembly. *J Cell Sci*. 115:2265-70.
Holzmann, K., C. Gerner, T. Korosec, A. Poltl, R. Grimm, and G. Sauermann. 1998. Identification and characterization of the ubiquitously occurring nuclear matrix protein NMP 238. *Biochem Biophys Res Commun*. 252:39-45.
Huang, S., L.I. Rothblum, and D. Chen. 2006. Ribosomal chromatin organization. *Biochem Cell Biol*. 84:444-9.
Chalfie, M., Y. Tu, G. Euskirchen, W.W. Ward, and D.C. Prasher. 1994. Green fluorescent protein as a marker for gene expression. *Science*. 263:802-5.
Chan, J.K., P.C. Park, and U. De Boni. 2000. Association of DNAse sensitive chromatin domains with the nuclear periphery in 3T3 cells in vitro. *Biochem Cell Biol*. 78:67-78.
Chen, D., M. Dundr, C. Wang, A. Leung, A. Lamond, T. Misteli, and S. Huang. 2005. Condensed mitotic chromatin is accessible to transcription factors and chromatin structural proteins. *J Cell Biol*. 168:41-54.
Chuang, C.H., and A.S. Belmont. 2007. Moving chromatin within the interphase nucleus-controlled transitions? *Semin Cell Dev Biol*. 18:698-706.
Chudakov, D.M., V.V. Belousov, A.G. Zaraisky, V.V. Novoselov, D.B. Staroverov, D.B. Zorov, S. Lukyanov, and K.A. Lukyanov. 2003. Kindling fluorescent proteins for precise in vivo photolabeling. *Nat Biotechnol*. 21:191-4.
Chudakov, D.M., V.V. Verkhusha, D.B. Staroverov, E.A. Souslova, S. Lukyanov, and K.A. Lukyanov. 2004. Photoswitchable cyan fluorescent protein for protein tracking. *Nat Biotechnol*. 22:1435-9.
Chudakov, D.M., S. Lukyanov, and K.A. Lukyanov. 2007. Using photoactivatable fluorescent protein Dendra2 to track protein movement. *Biotechniques*. 42:553, 555, 557 passim.
Jenuwein, T., and C.D. Allis. 2001. Translating the histone code. *Science*. 293:1074-80.
Jolly, C., L. Konecny, D.L. Grady, Y.A. Kutskova, J.J. Cotto, R.I. Morimoto, and C. Vourc'h. 2002. In vivo binding of active heat shock transcription factor 1 to human chromosome 9 heterochromatin during stress. *J Cell Biol*. 156:775-81.
Kalmárová, M., E. Smirnov, L. Kováčik, A. Popov, and I. Raška. 2008. Positioning of the NOR-bearing chromosomes in relation to nucleoli in daughter cells after mitosis. *Physiol. Res.* In press.
Kalmárová, M., E. Smirnov, M. Mašata, K. Koberna, A. Ligasová, A. Popov, and I. Raška. 2007. Positioning of NORs and NOR-bearing chromosomes in relation to nucleoli. *J Struct Biol*. 160:49-56.
Kanda, T., K.F. Sullivan, and G.M. Wahl. 1998. Histone-GFP fusion protein enables sensitive analysis of chromosome dynamics in living mammalian cells. *Curr Biol*. 8:377-85.
Khodjakov, A., and C.L. Rieder. 2006. Imaging the division process in living tissue culture cells. *Methods*. 38:2-16.
Kimura, H., and P.R. Cook. 2001. Kinetics of core histones in living human cells: little exchange of H3 and H4 and some rapid exchange of H2B. *J Cell Biol*. 153:1341-53.
King, T.H., W.A. Decatur, E. Bertrand, E.S. Maxwell, and M.J. Fournier. 2001. A well-connected and conserved nucleoplasmic helicase is required for production of box C/D and H/ACA snoRNAs and localization of snoRNP proteins. *Mol Cell Biol*. 21:7731-46.

Koberna, K., A. Ligasová, J. Malínský, A. Pliss, A.J. Siegel, Z. Cvačková, H. Fidlerová, M. Mašata, M. Fialová, I. Raška, and R. Berezney. 2005. Electron microscopy of DNA replication in 3-D: evidence for similar-sized replication foci throughout S-phase. *J Cell Biochem*. 94:126-38.

Koberna, K., J. Malínský, A. Pliss, M. Mašata, J. Večeřová, M. Fialová, J. Bednár, and I. Raška. 2002. Ribosomal genes in focus: new transcripts label the dense fibrillar components and form clusters indicative of "Christmas trees" in situ. *J Cell Biol*. 157:743-8.

Kouzarides, T. 2007. Chromatin modifications and their function. *Cell*. 128:693-705.

Kumaran, R.I., and D.L. Spector. 2008. A genetic locus targeted to the nuclear periphery in living cells maintains its transcriptional competence. *J Cell Biol*. 180:51-65.

Kumaran, R.I., R. Thakar, and D.L. Spector. 2008. Chromatin dynamics and gene positioning. *Cell*. 132:929-34.

Kupper, K., A. Kolbl, D. Biener, S. Dittrich, J. von Hase, T. Thormeyer, H. Fiegler, N.P. Carter, M.R. Speicher, T. Cremer, and M. Cremer. 2007. Radial chromatin positioning is shaped by local gene density, not by gene expression. *Chromosoma*. 116:285-306.

Kurakin, A. 2007. Self-organization versus Watchmaker: ambiguity of molecular recognition and design charts of cellular circuitry. *J Mol Recognit*. 20:205-14.

Lam, Y.W., L. Trinkle-Mulcahy, and A.I. Lamond. 2005. The nucleolus. *J Cell Sci*. 118:1335-7.

Lanctot, C., T. Cheutin, M. Cremer, G. Cavalli, and T. Cremer. 2007. Dynamic genome architecture in the nuclear space: regulation of gene expression in three dimensions. *Nat Rev Genet*. 8:104-15.

Leger, I., M. Guillaud, B. Krief, and G. Brugal. 1994. Interactive computer-assisted analysis of chromosome 1 colocalization with nucleoli. *Cytometry*. 16:313-23.

Leung, A.K., D. Gerlich, G. Miller, C. Lyon, Y.W. Lam, D. Lleres, N. Daigle, J. Zomerdijk, J. Ellenberg, and A.I. Lamond. 2004. Quantitative kinetic analysis of nucleolar breakdown and reassembly during mitosis in live human cells. *J Cell Biol*. 166:787-800.

Leung, A.K., L. Trinkle-Mulcahy, Y.W. Lam, J.S. Andersen, M. Mann, and A.I. Lamond. 2006. NOPdb: Nucleolar Proteome Database. *Nucleic Acids Res*. 34:D218-20.

Levenson, J.M., and J.D. Sweatt. 2005. Epigenetic mechanisms in memory formation. *Nat Rev Neurosci*. 6:108-18.

Lever, M.A., J.P. Th'ng, X. Sun, and M.J. Hendzel. 2000. Rapid exchange of histone H1.1 on chromatin in living human cells. *Nature*. 408:873-6.

Loizou, J.I., R. Murr, M.G. Finkbeiner, C. Sawan, Z.Q. Wang, and Z. Herceg. 2006. Epigenetic information in chromatin: the code of entry for DNA repair. *Cell Cycle*. 5:696-701.

Makino, Y., T. Mimori, C. Koike, M. Kanemaki, Y. Kurokawa, S. Inoue, T. Kishimoto, and T. Tamura. 1998. TIP49, homologous to the bacterial DNA helicase RuvB, acts as an autoantigen in human. *Biochem Biophys Res Commun*. 245:819-23.

Manuelidis, L., and J. Borden. 1988. Reproducible compartmentalization of individual chromosome domains in human CNS cells revealed by in situ hybridization and three-dimensional reconstruction. *Chromosoma*. 96:397-410.

Mateos-Langerak, J., S. Goetze, H. Leonhardt, T. Cremer, R. van Driel, and C. Lanctot. 2007. Nuclear architecture: Is it important for genome function and can we prove it? *J Cell Biochem*. 102:1067-75.

McKeegan, K.S., C.M. Debieux, S. Boulon, E. Bertrand, and N.J. Watkins. 2007. A dynamic scaffold of pre-snoRNP factors facilitates human box C/D snoRNP assembly. *Mol Cell Biol*. 27:6782-93.

McNally, J.G., T. Karpova, J. Cooper, and J.A. Conchello. 1999. Three-dimensional imaging by deconvolution microscopy. *Methods*. 19:373-85.

Meaburn, K.J., T. Misteli, and E. Soutoglou. 2007. Spatial genome organization in the formation of chromosomal translocations. *Semin Cancer Biol*. 17:80-90.

Meyer zum Buschenfelde, D., R. Tauber, and O. Huber. 2006. TFF3-peptide increases transepithelial resistance in epithelial cells by modulating claudin-1 and -2 expression. *Peptides*. 27:3383-90.

Miller, O.L., Jr., and B.R. Beatty. 1969. Visualization of nucleolar genes. *Science*. 164:955-7.

Misteli, T. 2001. Protein dynamics: implications for nuclear architecture and gene expression. *Science*. 291:843-7.

Misteli, T. 2007. Beyond the sequence: cellular organization of genome function. *Cell*. 128:787-800.

Misteli, T., A. Gunjan, R. Hock, M. Bustin, and D.T. Brown. 2000. Dynamic binding of histone H1 to chromatin in living cells. *Nature*. 408:877-81.

Nagele, R.G., T. Freeman, L. McMorrow, Z. Thomson, K. Kitson-Wind, and H. Lee. 1999. Chromosomes exhibit preferential positioning in nuclei of quiescent human cells. *J Cell Sci*. 112 (Pt 4):525-35.

Nakano, A. 2002. Spinning-disk confocal microscopy -- a cutting-edge tool for imaging of membrane traffic. *Cell Struct Funct*. 27:349-55.

Nikiforova, M.N., J.R. Stringer, R. Blough, M. Medvedovic, J.A. Fagin, and Y.E. Nikiforov. 2000. Proximity of chromosomal loci that participate in radiation-induced rearrangements in human cells. *Science*. 290:138-41.

Nunez, E., Y.S. Kwon, K.R. Hutt, Q. Hu, M.D. Cardamone, K.A. Ohgi, I. Garcia-Bassets, D.W. Rose, C.K. Glass, M.G. Rosenfeld, and X.D. Fu. 2008a. Nuclear receptor-enhanced transcription requires motor- and LSD1-dependent gene networking in interchromatin granules. *Cell*. 132:996-1010.

Nunez, E., Y.S. Kwon, K.R. Hutt, Q. Hu, M.D. Cardamone, K.A. Ohgi, I. Garcia-Bassets, D.W. Rose, C.K. Glass, M.G. Rosenfeld, and X.D. Fu. 2008b. Nuclear receptor-enhanced transcription requires motor- and LSD1-dependent gene networking in interchromatin granules. *Cell*. 134:189.

Ogushi, S., C. Palmieri, H. Fulka, M. Saitou, T. Miyano, and J. Fulka, Jr. 2008. The maternal nucleolus is essential for early embryonic development in mammals. *Science*. 319:613-6.

Osborne, C.S., L. Chakalova, K.E. Brown, D. Carter, A. Horton, E. Debrand, B. Goyenechea, J.A. Mitchell, S. Lopes, W. Reik, and P. Fraser. 2004. Active genes dynamically colocalize to shared sites of ongoing transcription. *Nat Genet*. 36:1065-71.

Parada, L., and T. Misteli. 2002. Chromosome positioning in the interphase nucleus. *Trends Cell Biol*. 12:425-32.

Parada, L.A., P.G. McQueen, and T. Misteli. 2004. Tissue-specific spatial organization of genomes. *Genome Biol*. 5:R44.

Parada, L.A., P.G. McQueen, P.J. Munson, and T. Misteli. 2002. Conservation of relative chromosome positioning in normal and cancer cells. *Curr Biol*. 12:1692-7.

Parada, L.A., J.J. Roix, and T. Misteli. 2003. An uncertainty principle in chromosome positioning. *Trends Cell Biol*. 13:393-6.

Patterson, G.H., and J. Lippincott-Schwartz. 2002. A photoactivatable GFP for selective photolabeling of proteins and cells. *Science*. 297:1873-7.

Peng, J.C., and G.H. Karpen. 2007. H3K9 methylation and RNA interference regulate nucleolar organization and repeated DNA stability. *Nat Cell Biol*. 9:25-35.

Pinkel, D., T. Straume, and J.W. Gray. 1986. Cytogenetic analysis using quantitative, high-sensitivity, fluorescence hybridization. *Proc Natl Acad Sci U S A*. 83:2934-8.

Pombo, A., P. Cuello, W. Schul, J.B. Yoon, R.G. Roeder, P.R. Cook, and S. Murphy. 1998. Regional and temporal specialization in the nucleus: a transcriptionally-active nuclear domain rich in PTF, Oct1 and PIKA antigens associates with specific chromosomes early in the cell cycle. *Embo J*. 17:1768-78.

Prasher, D.C., V.K. Eckenrode, W.W. Ward, F.G. Prendergast, and M.J. Cormier. 1992. Primary structure of the Aequorea victoria green-fluorescent protein. *Gene*. 111:229-33.

Rabl, C. 1885. Űber Zelltheilung. *Morphologisches Jahrbuch* 10:214-330.

Raška, I. 2003. Oldies but goldies: searching for Christmas trees within the nucleolar architecture. *Trends Cell Biol*. 13:517-25.

Raška, I., M. Dundr, K. Koberna, I. Melčák, M.C. Risueno, and I. Torok. 1995. Does the synthesis of ribosomal RNA take place within nucleolar fibrillar centers or dense fibrillar components? A critical appraisal. *J Struct Biol*. 114:1-22.

Raška, I., K. Koberna, J. Malínský, H. Fidlerová, and M. Mašata. 2004. The nucleolus and transcription of ribosomal genes. *Biol Cell*. 96:579-94.

Raška, I., P.J. Shaw, and D. Cmarko. 2006a. New insights into nucleolar architecture and activity. *Int Rev Cytol*. 255:177-235.

Raška, I., P.J. Shaw, and D. Cmarko. 2006b. Structure and function of the nucleolus in the spotlight. *Curr Opin Cell Biol*. 18:325-34.

Redon, C., D. Pilch, E. Rogakou, O. Sedelnikova, K. Newrock, and W. Bonner. 2002. Histone H2A variants H2AX and H2AZ. *Curr Opin Genet Dev*. 12:162-9.

Roix, J.J., P.G. McQueen, P.J. Munson, L.A. Parada, and T. Misteli. 2003. Spatial proximity of translocation-prone gene loci in human lymphomas. *Nat Genet*. 34:287-91.

Rust, M.J., M. Bates, and X. Zhuang. 2006. Sub-diffraction-limit imaging by stochastic optical reconstruction microscopy (STORM). *Nat Methods*. 3:793-5.

Salzer, U., M. Kubicek, and R. Prohaska. 1999. Isolation, molecular characterization, and tissue-specific expression of ECP-51 and ECP-54 (TIP49), two homologous, interacting erythroid cytosolic proteins. *Biochim Biophys Acta*. 1446:365-70.

Santoro, R., J. Li, and I. Grummt. 2002. The nucleolar remodeling complex NoRC mediates heterochromatin formation and silencing of ribosomal gene transcription. *Nat Genet*. 32:393-6.

Savino, T.M., J. Gebrane-Younes, J. De Mey, J.B. Sibarita, and D. Hernandez-Verdun. 2001. Nucleolar assembly of the rRNA processing machinery in living cells. *J Cell Biol*. 153:1097-110.

Shagin, D.A., E.V. Barsova, Y.G. Yanushevich, A.F. Fradkov, K.A. Lukyanov, Y.A. Labas, T.N. Semenova, J.A. Ugalde, A. Meyers, J.M. Nunez, E.A. Widder, S.A. Lukyanov, and M.V. Matz. 2004. GFP-like proteins as ubiquitous metazoan superfamily: evolution of functional features and structural complexity. *Mol Biol Evol*. 21:841-50.

Shiels, C., S.A. Islam, R. Vatcheva, P. Sasieni, M.J. Sternberg, P.S. Freemont, and D. Sheer. 2001. PML bodies associate specifically with the MHC gene cluster in interphase nuclei. *J Cell Sci*. 114:3705-16.

Shimomura, O., F.H. Johnson, and Y. Saiga. 1962. Extraction, purification and properties of aequorin, a bioluminescent protein from the luminous hydromedusan, Aequorea. *J Cell Comp Physiol*. 59:223-39.

Schardin, M., T. Cremer, H.D. Hager, and M. Lang. 1985. Specific staining of human chromosomes in Chinese hamster x man hybrid cell lines demonstrates interphase chromosome territories. *Hum Genet*. 71:281-7.

Schul, W., I. van Der Kraan, A.G. Matera, R. van Driel, and L. de Jong. 1999. Nuclear domains enriched in RNA 3'-processing factors associate with coiled bodies and histone genes in a cell cycle-dependent manner. *Mol Biol Cell*. 10:3815-24.

Smetana, K. 2002. Structural features of nucleoli in blood, leukemic, lymphoma and myeloma cells. *Eur J Histochem*. 46:125-32.

Smirnov, E., M. Kalmárová, K. Koberna, Z. Zemanová, J. Malínský, M. Mašata, Z. Cvačková, K. Michalová, and I. Raška. 2006. NORs and their transcription competence during the cell cycle. *Folia Biol (Praha)*. 52:59-70.

Spector, D.L. 2001. Nuclear domains. *J Cell Sci*. 114:2891-3.

Staněk, D., S.D. Rader, M. Klingauf, and K.M. Neugebauer. 2003. Targeting of U4/U6 small nuclear RNP assembly factor SART3/p110 to Cajal bodies. *J Cell Biol*. 160:505-16.

Sun, H.B., J. Shen, and H. Yokota. 2000. Size-dependent positioning of human chromosomes in interphase nuclei. *Biophys J*. 79:184-90.

Tanabe, H., F.A. Habermann, I. Solovei, M. Cremer, and T. Cremer. 2002. Non-random radial arrangements of interphase chromosome territories: evolutionary considerations and functional implications. *Mutat Res*. 504:37-45.

Taubert, S., C. Gorrini, S.R. Frank, T. Parisi, M. Fuchs, H.M. Chan, D.M. Livingston, and B. Amati. 2004. E2F-dependent histone acetylation and recruitment of the Tip60 acetyltransferase complex to chromatin in late G1. *Mol Cell Biol*. 24:4546-56.

Thomson, I., S. Gilchrist, W.A. Bickmore, and J.R. Chubb. 2004. The radial positioning of chromatin is not inherited through mitosis but is established de novo in early G1. *Curr Biol*. 14:166-72.

Trinkle-Mulcahy, L., and A.I. Lamond. 2008. Nuclear functions in space and time: Gene expression in a dynamic, constrained environment. *FEBS Lett*. 582:1960-70.

Tsien, R.Y. 1998. The green fluorescent protein. *Annu Rev Biochem*. 67:509-44.

Tsutsui, H., S. Karasawa, H. Shimizu, N. Nukina, and A. Miyawaki. 2005. Semi-rational engineering of a coral fluorescent protein into an efficient highlighter. *EMBO Rep*. 6:233-8.

Venteicher, A.S., Z. Meng, P.J. Mason, T.D. Veenstra, and S.E. Artandi. 2008. Identification of ATPases pontin and reptin as telomerase components essential for holoenzyme assembly. *Cell*. 132:945-57.

Verkade, P. 2008. Moving EM: the Rapid Transfer System as a new tool for correlative light and electron microscopy and high throughput for high-pressure freezing. *J Microsc*. 230:317-28.

Verkhusha, V.V., and A. Sorkin. 2005. Conversion of the monomeric red fluorescent protein into a photoactivatable probe. *Chem Biol*. 12:279-85.

Visser, A.E., and J.A. Aten. 1999. Chromosomes as well as chromosomal subdomains constitute distinct units in interphase nuclei. *J Cell Sci*. 112 (Pt 19):3353-60.

Volpi, E.V., E. Chevret, T. Jones, R. Vatcheva, J. Williamson, S. Beck, R.D. Campbell, M. Goldsworthy, S.H. Powis, J. Ragoussis, J. Trowsdale, and D. Sheer. 2000. Large-scale chromatin organization of the major histocompatibility complex and other regions of human chromosome 6 and its response to interferon in interphase nuclei. *J Cell Sci*. 113 (Pt 9):1565-76.

Walter, J., L. Schermelleh, M. Cremer, S. Tashiro, and T. Cremer. 2003. Chromosome order in HeLa cells changes during mitosis and early G1, but is stably maintained during subsequent interphase stages. *J Cell Biol*. 160:685-97.

Watkins, N.J., A. Dickmanns, and R. Luhrmann. 2002. Conserved stem II of the box C/D motif is essential for nucleolar localization and is required, along with the 15.5K protein, for the hierarchical assembly of the box C/D snoRNP. *Mol Cell Biol*. 22:8342-52.

Watkins, N.J., I. Lemm, D. Ingelfinger, C. Schneider, M. Hossbach, H. Urlaub, and R. Luhrmann. 2004. Assembly and maturation of the U3 snoRNP in the nucleoplasm in a large dynamic multiprotein complex. *Mol Cell*. 16:789-98.

Weiske, J., and O. Huber. 2005. The histidine triad protein Hint1 interacts with Pontin and Reptin and inhibits TCF-beta-catenin-mediated transcription. *J Cell Sci*. 118:3117-29.

Weiske, J., and O. Huber. 2006. The histidine triad protein Hint1 triggers apoptosis independent of its enzymatic activity. *J Biol Chem*. 281:27356-66.

Wiedenmann, J., S. Ivanchenko, F. Oswald, F. Schmitt, C. Rocker, A. Salih, K.D. Spindler, and G.U. Nienhaus. 2004. EosFP, a fluorescent marker protein with UV-inducible green-to-red fluorescence conversion. *Proc Natl Acad Sci U S A*. 101:15905-10.

Wiesmeijer, K., I.M. Krouwels, H.J. Tanke, and R.W. Dirks. 2008. Chromatin movement visualized with photoactivable GFP-labeled histone H4. *Differentiation*. 76:83-90.

Williams, R.R., S. Broad, D. Sheer, and J. Ragoussis. 2002. Subchromosomal positioning of the epidermal differentiation complex (EDC) in keratinocyte and lymphoblast interphase nuclei. *Exp Cell Res*. 272:163-75.

Williams, R.R., and A.G. Fisher. 2003. Chromosomes, positions please! *Nat Cell Biol*. 5:388-90.

Wood, M.A., S.B. McMahon, and M.D. Cole. 2000. An ATPase/helicase complex is an essential cofactor for oncogenic transformation by c-Myc. *Mol Cell*. 5:321-30.

Yang, J.M., S.J. Baserga, S.J. Turley, and K.M. Pollard. 2001. Fibrillarin and other snoRNP proteins are targets of autoantibodies in xenobiotic-induced autoimmunity. *Clin Immunol*. 101:38-50.

Zaros, C., J.F. Briand, Y. Boulard, S. Labarre-Mariotte, M.C. Garcia-Lopez, P. Thuriaux, and F. Navarro. 2007. Functional organization of the Rpb5 subunit shared by the three yeast RNA polymerases. *Nucleic Acids Res*. 35:634-47.

Zink, D., T. Cremer, R. Saffrich, R. Fischer, M.F. Trendelenburg, W. Ansorge, and E.H. Stelzer. 1998. Structure and dynamics of human interphase chromosome territories in vivo. *Hum Genet*. 102:241-51.